# PTF10iya: a short-lived, luminous flare from the nuclear region of a star-forming galaxy

S. Bradley Cenko,[1]★ Joshua S. Bloom,[1] S. R. Kulkarni,[2] Linda E. Strubbe,[1,3]
Adam A. Miller,[1] Nathaniel R. Butler,[1]† Robert M. Quimby,[4] Avishay Gal-Yam,[5]
Eran O. Ofek,[2]† Eliot Quataert,[1,3] Lars Bildsten,[6,7] Dovi Poznanski,[1,8,9]†
Daniel A. Perley,[1] Adam N. Morgan,[1] Alexei V. Filippenko,[1] Dale A. Frail,[10]
Iair Arcavi,[5] Sagi Ben-Ami,[5] Antonio Cucchiara,[1,8] Christopher D. Fassnacht,[11]
Yoav Green,[5] Isobel M. Hook,[12,13] D. Andrew Howell,[6,14] David J. Lagattuta,[11]
Nicholas M. Law,[15] Mansi M. Kasliwal,[2] Peter E. Nugent,[8] Jeffrey M. Silverman,[1]
Mark Sullivan,[12] Shriharsh P. Tendulkar[2] and Ofer Yaron[5]

[1]*Department of Astronomy, University of California, Berkeley, CA 94720-3411, USA*
[2]*Cahill Center for Astrophysics, California Institute of Technology, Pasadena, CA 91125, USA*
[3]*Theoretical Astrophysics Center, University of California, Berkeley, CA 94720-3411, USA*
[4]*IPMU, University of Tokyo, Kashiwanoha 5-1-5, Kashiwa-shi, Chiba, Japan*
[5]*Department of Particle Physics and Astrophysics, The Weizmann Institute of Science, Rehovot 76100, Israel*
[6]*Department of Physics, Broida Hall, University of California, Santa Barbara, CA 93106, USA*
[7]*The Kavli Institute for Theoretical Physics, Kohn Hall, University of California, Santa Barbara, CA 93106, USA*
[8]*Computational Cosmology Center, Lawrence Berkeley National Laboratory, 1 Cyclotron Road, Berkeley, CA 94720, USA*
[9]*School of Physics and Astronomy, Tel-Aviv University, Tel-Aviv 69978, Israel*
[10]*National Radio Astronomy Observatory, PO Box 0, Socorro, NM 87801, USA*
[11]*Department of Physics, University of California Davis, 1 Shields Avenue, Davis, CA 95616, USA*
[12]*Department of Physics (Astrophysics), University of Oxford, Keble Road, Oxford OX1 3RH*
[13]*INAF-Osservatorio di Roma, via Frascati 33, I-00040 Monteporzio Catone (Roma), Italy*
[14]*Las Cumbres Observatory Global Telescope Network, Goleta, CA 93117, USA*
[15]*Dunlap Institute for Astronomy and Astrophysics, University of Toronto, 50 St. George Street, Toronto M5S 3H4, Ontario, Canada*

## ABSTRACT

We present the discovery and characterization of PTF10iya, a short-lived ($\Delta t \approx 10$ d, with an optical decay rate of $\sim 0.3$ mag d$^{-1}$), luminous ($M_{g'} \approx -21$ mag) transient source found by the Palomar Transient Factory. The ultraviolet/optical spectral energy distribution is reasonably well fitted by a blackbody with $T \approx (1–2) \times 10^4$ K and peak bolometric luminosity $L_{BB} \approx (1–5) \times 10^{44}$ erg s$^{-1}$ (depending on the details of the extinction correction). A comparable amount of energy is radiated in the X-ray band that appears to result from a distinct physical process. The location of PTF10iya is consistent with the nucleus of a star-forming galaxy ($z = 0.224\,05 \pm 0.000\,06$) to within 350 mas (99.7 per cent confidence radius), or a projected distance of less than 1.2 kpc. At first glance, these properties appear reminiscent of the characteristic 'big blue bump' seen in the near-ultraviolet spectra of many active galactic nuclei (AGNs). However, emission-line diagnostics of the host galaxy, along with a historical light curve extending back to 2007, show no evidence for AGN-like activity. We therefore consider whether the tidal disruption of a star by an otherwise quiescent supermassive black hole may account for our observations. Though with limited temporal information, PTF10iya appears broadly consistent with the predictions for the early 'super-Eddington' phase of a

★E-mail: cenko@astro.berkeley.edu
†Einstein Fellow.

solar-type star being disrupted by a $\sim 10^7\,\mathrm{M}_\odot$ black hole. Regardless of the precise physical origin of the accreting material, the large luminosity and short duration suggest that otherwise quiescent galaxies can transition extremely rapidly to radiate near the Eddington limit; many such outbursts may have been missed by previous surveys lacking sufficient cadence.

**Key words:** accretion, accretion discs – black hole physics – galaxies: active – galaxies: nuclei.

# 1 INTRODUCTION

Understanding the physics of accretion, and, in particular, the associated electromagnetic emission, is a topic at the forefront of modern astrophysics. From planet formation to Galactic X-ray binaries to the most luminous quasars, accretion plays a role in an astounding array of phenomena across a diverse range of mass and size scales. Of special interest is the importance of the process in the formation and growth of the supermassive black holes (SMBHs) that appear to reside in the centres of all bulge galaxies (Kormendy & Richstone 1995), and the mechanism by which these SMBHs are intimately connected to the growth and evolution of galaxies (i.e. the $M_{\rm BH}$–$\sigma_*$ relation; Ferrarese & Merritt 2000; Gebhardt et al. 2000).

Rees (1988) first suggested that the tidal disruption of a star by a SMBH could be a powerful method to study accretion in otherwise quiescent galaxies. If the observational signature of the resulting electromagnetic emission, known as a tidal disruption flare (TDF), were better constrained, these outbursts could potentially be used to probe the properties (i.e. mass) of SMBHs in quiescent galaxies beyond the reach of (resolved) kinematic studies of central gas and stars.

The task of observationally identifying TDFs, however, is greatly complicated by the diverse array of transient phenomena that occur in galactic nuclei. Aside from the well-known classes of active galactic nuclei (AGNs), such as blazars and normal Seyfert galaxies, potential TDF 'impostors' include the relatively rare double-peaked emitters (systems that exhibit both blueshifted and redshifted emission lines that may indicate an origin in a rotating accretion disc; Halpern & Filippenko 1988), and Type IIn supernovae (SNe IIn; objects with narrow and intermediate width emission lines indicative of interaction with a moderately dense circumstellar medium; see Filippenko 1997 for a review). Future progress requires a full accounting of these interlopers, both at the individual (i.e. to establish or rule out a TDF origin for a given event) and class (i.e. for rate calculations) levels (van Velzen et al. 2011a; Strubbe & Quataert 2011).

In the optical bandpass, wide-field, high-cadence surveys such as the Palomar Transient Factory (PTF; Law et al. 2009; Rau et al. 2009), Pan-STARRS1 (PS1; Kaiser et al. 2002), the Catalina Real-time Transient Survey (CRTS; Drake et al. 2009) and SkyMapper (Schmidt et al. 2005) are all currently attempting to chart the bright end of the transient landscape in advance of the Large Synoptic Survey Telescope (LSST). As untargeted transient surveys, these projects should provide a relatively unbiased view (with the notable exception of dust extinction) of the optical variability of nearby galaxies, where many AGNs and SNe emit a significant fraction of their bolometric luminosity, and are therefore well suited to address many of the questions mentioned above.

Here we present the discovery by PTF of a short-lived, luminous transient (PTF10iya) in the nuclear region of a redshift $z = 0.22$ star-forming galaxy, which serves as an interesting test case for many of these issues. Our manuscript is organized as follows.

In Section 2, we describe the discovery of PTF10iya, as well as optical, ultraviolet (UV), near-infrared (NIR) and X-ray follow-up observations and archival data at the location of the transient. Section 3 presents the astrometry of the transient emission, the broad-band spectral energy distribution (SED), and the properties of the host galaxy. In Section 4, we outline possible emission mechanisms to explain the observed properties of the outburst.

Throughout this paper, we adopt a standard $\Lambda$ cold dark matter cosmology with $H_0 = 71\,\mathrm{km\,s^{-1}\,Mpc^{-1}}$, $\Omega_{\rm m} = 0.27$ and $\Omega_\Lambda = 1 - \Omega_{\rm m} = 0.73$ (Spergel et al. 2007). All quoted uncertainties are $1\sigma$ (68 per cent) confidence intervals unless otherwise noted, and UT times are used throughout.

# 2 OBSERVATIONS

## 2.1 Palomar 48-inch discovery and photometry

As part of the PTF 5-d cadence survey, we obtained a pair of $R$-band images of PTF field 4328 on 2010 June 6 with the Palomar 48-inch telescope (P48) equipped with the refurbished CFHT12k camera (Rahmer et al. 2008). Subtraction of a stacked reference image of the field with HOTPANTS[1] revealed a new transient source at coordinates $\alpha = 14^{\rm h}38^{\rm m}41\fs00$, $\delta = 37°39'33\farcs6$ (J2000.0), with an astrometric uncertainty of $\pm150$ mas in each coordinate [referenced with respect to the Sloan Digital Sky Survey (SDSS) Data Release 7 catalogue; Abazajian et al. 2009].
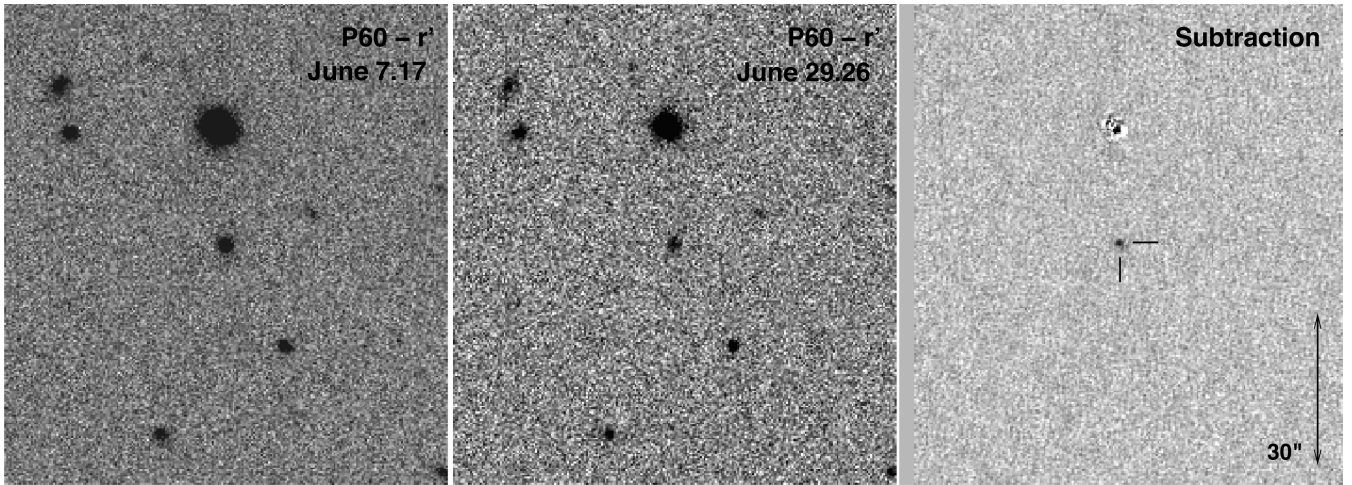
The transient was discovered 3 hours later by OARICAL, an autonomous software framework of the PTF collaboration (Bloom et al. 2011b), and given the name PTF10iya. The software further noted the presence of a coincident catalogued extended source, SDSS J143840.98+373933.4 (hereafter SDSS J1438; Fig. 1), identifying this object as a potential host galaxy for PTF10iya.

No transient emission was detected at this location with P48, either prior to (extending back to 2009 May) or after (through 2011 July) the outburst, to a typical $3\sigma$ limiting magnitude of $R \approx 21$. A listing of P48 observations taken around the time of outburst, calibrated using SDSS magnitudes of nearby point sources and the filter transformations of Jordi, Grebel & Ammon (2006), is provided in Table 1.

This field was also observed as part of the Palomar-QUEST survey (Djorgovski et al. 2008) on eight separate nights ranging from 2007 May 6 to 2008 July 30. The observations have been compiled into a single searchable data base at the Lawrence Berkeley National Laboratory as part of the Deep Sky project.[2] The galaxy SDSS J1438 is only weakly detected in most images. We therefore forgo image subtraction and perform photometry with a 2.5 arcsec (radius) aperture on all individual frames, using the SDSS $i'$ filter to

---

[1] See http://www.astro.washington.edu/users/becker/hotpants.html.
[2] See http://supernova.lbl.gov/~nugent/deepsky.html.

**Figure 1.** Finder chart for PTF10iya. Left-hand panel: P60 $r'$ image from 2010 June 7. Middle panel: P60 reference image from several weeks later. Right-hand panel: digital subtraction of the two P60 images. The transient PTF10iya is indicated by the black tick marks. All images are oriented with north up and east to the left.

**Table 1.** UV/optical observations of PTF10iya.

| Date[a] (UT) | Telescope/instrument | Filter | Exposure time (s) | Magnitude[b] |
|---|---|---|---|---|
| 2010 June 1.295 | P48 | $R$ | 60.0 | >20.62 |
| 2010 June 1.344 | P48 | $R$ | 60.0 | >20.53 |
| 2010 June 6.302 | P48 | $R$ | 60.0 | $19.77 \pm 0.10$ |
| 2010 June 6.356 | P48 | $R$ | 60.0 | $19.91 \pm 0.11$ |
| 2010 June 7.170 | P60 | $i'$ | 120.0 | $20.24 \pm 0.20$ |
| 2010 June 7.172 | P60 | $r'$ | 120.0 | $19.92 \pm 0.10$ |
| 2010 June 7.174 | P60 | $g'$ | 120.0 | $19.79 \pm 0.08$ |
| 2010 June 11.335 | P48 | $R$ | 60.0 | >19.39 |
| 2010 June 11.779 | *Swift*/UVOT | $UVW1$ | 314.5 | $19.73 \pm 0.27$ |
| 2010 June 11.782 | *Swift*/UVOT | $U$ | 157.0 | $19.31 \pm 0.18$ |
| 2010 June 11.784 | *Swift*/UVOT | $UVW2$ | 629.4 | $19.73 \pm 0.17$ |
| 2010 June 11.788 | *Swift*/UVOT | $UVM2$ | 1478.2 | $19.77 \pm 0.15$ |
| 2010 June 13.311 | P60 | $i'$ | 180.0 | $22.14 \pm 0.35$ |
| 2010 June 13.313 | P60 | $r'$ | 120.0 | $21.62 \pm 0.28$ |
| 2010 June 13.318 | P60 | $g'$ | 120.0 | $21.46 \pm 0.28$ |
| 2010 June 16.334 | P48 | $R$ | 60.0 | >20.75 |
| 2010 June 16.378 | P48 | $R$ | 60.0 | >20.60 |
| 2010 June 18.687 | P60 | $i'$ | 1080.0 | >22.24 |
| 2010 June 18.689 | P60 | $r'$ | 720.0 | >22.69 |
| 2010 June 18.689 | P60 | $g'$ | 360.0 | >21.61 |
| 2010 August 10.498 | *Swift*/UVOT | $UVM2$ | 1771.4 | >21.01 |
| 2010 August 10.499 | *Swift*/UVOT | $U$ | 591.4 | >20.67 |
| 2010 August 10.499 | *Swift*/UVOT | $UVW1$ | 1179.0 | >20.47 |
| 2010 August 10.499 | *Swift*/UVOT | $UVW2$ | 1998.5 | >20.69 |

[a] UT at the mid-point of exposure/co-add.
[b] All reported magnitudes have had host-galaxy flux removed and represent light only from the transient PTF10iya. Magnitudes here have not been corrected for Galactic extinction [$E(B - V) = 0.010$ mag; Schlegel et al. 1998], nor for extinction in the host galaxy of the transient. Observations in the $g'$, $r'$, and $i'$ bands are reported on the AB magnitude system (Oke & Gunn 1983). $U$- and $R$-band observations are with reference to Vega, while $UVW1$, $UVM2$ and $UVW2$ are on the UVOT photometric system (Poole et al. 2008).

calibrate the observed red bandpass (an order-blocking filter with a cut-off bluewards of $\lambda \approx 6100$ Å). The resulting photometry is given in Table 2.

Taking the weighted mean of all the pre-outburst Deep Sky measurements of the potential host galaxy, we calculate $\langle i' \rangle = 19.53 \pm$ 0.17 mag, in good agreement with the value from SDSS, given the somewhat different passbands ($i'_{\rm SDSS} = 19.65 \pm 0.04$ mag). If we assume a constant flux equal to this value, we find $\chi^2 = 6.32$ (17 d.o.f.). The observations are therefore consistent with a static flux level (null probability 0.991).

**Table 2.** Historical Deep Sky observations of SDSS J1438.

| Date[a] (UT) | Exposure time (s) | Magnitude[b] |
|---|---|---|
| 2007 May 6.486 | 60.4 | 19.84 ± 0.31 |
| 2007 May 18.462 | 60.2 | 19.63 ± 0.30 |
| 2007 May 18.464 | 60.4 | 19.72 ± 0.31 |
| 2007 May 18.476 | 60.5 | 19.82 ± 0.33 |
| 2007 May 18.477 | 60.4 | 19.73 ± 0.31 |
| 2008 May 8.476 | 60.2 | 19.60 ± 0.24 |
| 2008 May 8.477 | 60.4 | 19.41 ± 0.27 |
| 2008 May 8.485 | 60.3 | 19.66 ± 0.27 |
| 2008 May 8.486 | 60.3 | 19.30 ± 0.40 |
| 2008 Jun 10.326 | 60.3 | 19.34 ± 0.26 |
| 2008 Jun 10.368 | 60.3 | 19.61 ± 0.32 |
| 2008 Jun 13.306 | 80.5 | 19.61 ± 0.30 |
| 2008 Jun 13.351 | 80.3 | 19.42 ± 0.29 |
| 2008 Jun 18.239 | 100.3 | 19.62 ± 0.34 |
| 2008 Jul 2.286 | 100.3 | 19.41 ± 0.29 |
| 2008 Jul 2.317 | 100.4 | 19.55 ± 0.29 |
| 2008 Jul 30.194 | 100.3 | 19.29 ± 0.23 |
| 2008 Jul 30.238 | 100.3 | 19.32 ± 0.26 |

[a] UT at the mid-point of exposure.

[b] Instrumental magnitudes were determined using a 2.5 arcsec (radius) aperture. Photometric calibration was performed relative to the SDSS $i'$ filter and are on the AB magnitude system (Oke & Gunn 1983). The magnitudes here have not been corrected for Galactic extinction [$E(B - V) = 0.010$ mag; Schlegel, Finkbeiner & Davis 1998], nor for extinction in the host galaxy.

We caution, however, that an outburst of comparable magnitude to that observed from PTF10iya ($i' = 20.24$ mag; Section 2.2) may not have been detectable due to the small ratio of host flux to transient flux and the low signal-to-noise ratio of most observations. The above limits therefore more directly limit brighter and/or redder outbursts from SDSS J1438.

## 2.2 Palomar 60-inch photometry

Upon discovery of PTF10iya, the field was automatically inserted into the queue of the robotic Palomar 60-inch telescope (P60; Cenko et al. 2006) for multicolour follow-up observations. Images were processed using our custom real-time pipeline, and then subtracted from reference frames obtained several months after the outburst using HOTPANTS (Fig. 1). Subtracting late-time (after 2010 July) P60 images from archival SDSS frames yielded no residual flux, confirming that the transient was below our detection threshold at this time. A log of our P60 observations of PTF10iya, with later images stacked to increase depth, is provided in Table 1.

## 2.3 *Swift* UV-Optical Telescope/X-ray Telescope

Motivated by the blue continuum (Section 2.6) and the large absolute magnitude of the outburst ($M_R \approx -21$ mag; Section 3.2), we triggered UV and X-ray target-of-opportunity observations of PTF10iya with the *Swift* satellite (Gehrels et al. 2004). The field was observed by the UV–Optical Telescope (UVOT; Roming et al. 2005) and the X-ray Telescope (XRT; Burrows et al. 2005) beginning at 17:53 on 2010 June 11. A second set of images were obtained with *Swift* on 2010 August 10, while a series of reference orbits observed from 2011 August 18 to 2011 September 7 were stacked to remove quiescent flux from the potential host galaxy SDSS J1438.

For the UVOT $U$-band observations, we determined the count rate at the location of PTF10iya using the techniques described

by Li et al. (2006), while for the *UVW*1, *UVM*2 and *UVW*2 data we used the methods of Poole et al. (2008).[3] After subtracting the pile-up-corrected count rates directly (see e.g. Brown et al. 2009), transient emission at the location of PTF10iya is clearly detected in all four blue filters in our initial epoch on 2010 June 11. Comparing our second epoch on 2010 August 10 with the late-time reference images, we find that the UV flux has not varied over this interval. This would suggest that the transient emission has faded below the UVOT sensitivity limit several months after discovery. A full listing of the host-subtracted UV photometry is provided in Table 1.

We reduced the XRT data using the pipeline described by Butler (2007). In the first epoch on 2010 June 11, an X-ray source is clearly detected ($34.5 \pm 4.5$ counts) at the location of PTF10iya (though with large astrometric uncertainty, $\sim5$ arcsec), corresponding to a flux $F_X = (7.5^{+6.2}_{-2.5}) \times 10^{-13}$ erg cm$^{-2}$ s$^{-1}$ (0.3–10 keV). Fitting a power-law model (d$N$/d$E \propto E^{-\Gamma}$) to the observed spectrum results in a photon index of $\Gamma = 1.8^{+1.2}_{-1.0}$ ($\chi^2 = 14.72$ for 17 d.o.f.). No X-ray emission is detected at the location of PTF10iya in the second epoch obtained on 2010 August 10, nor in the final reference epoch from 2011 August to September. Assuming the same spectrum as in the first epoch, we derive a $3\sigma$ flux limit (0.3–10 keV) on the quiescent flux level of $F_X < 3 \times 10^{-14}$ erg cm$^{-2}$ s$^{-1}$.

## 2.4 Keck laser guide-star adaptive optics

On 2010 June 18, we observed the field of PTF10iya with the Near-Infrared Camera 2 (NIRC2) mounted behind the laser guide-star adaptive optics (LGS/AO) system on the Keck II telescope (Wizinowich et al. 2006). Beginning at 8:10, we obtained a series of $K'$-band exposures, each consisting of 10 non-destructive readouts of either 10 or 20 s, for a total time on source of 800 s. Images were reduced using standard IRAF[4] routines, using a median combination of the (non-aligned) dithered images to correct for the sky background. Prior to registration, we applied the distortion correction provided by the Keck Observatory.[5] The resulting image (shown in the middle and right-hand panels of Fig. 2) was used for astrometric analysis (Section 3.1). However, this procedure does not conserve flux, and so we created a separate co-addition that did not include the distortion correction for photometry.

A second series of LGS/AO images were obtained on 2010 December 2 with a total integration time of 750 s using the identical instrumental setup. Both SDSS J1438 and the offset point source (Section 3.1) are detected, with no evidence for variability in either source.

## 2.5 Palomar 200-inch Large Format Camera

We observed the field of PTF10iya with the Large Format Camera (LFC; Simcoe et al. 2000) mounted on the 5-m Palomar Hale Telescope on 2010 August 9. A total of five dithered exposures (each 120 s) were obtained in the $r'$ filter beginning at 4:46. After registering the individual images to a common reference, the frames

---

[3] We do not use the $V$-band and $B$-band data here, as the host plus transient were only marginally detected, and no *Swift* reference frames were obtained in these filters.

[4] IRAF is distributed by the National Optical Astronomy Observatory, which is operated by the Association for Research in Astronomy, Inc., under cooperative agreement with the National Science Foundation.

[5] See http://www2.keck.hawaii.edu/inst/nirc2/forReDoc/post_observing/dewarp.
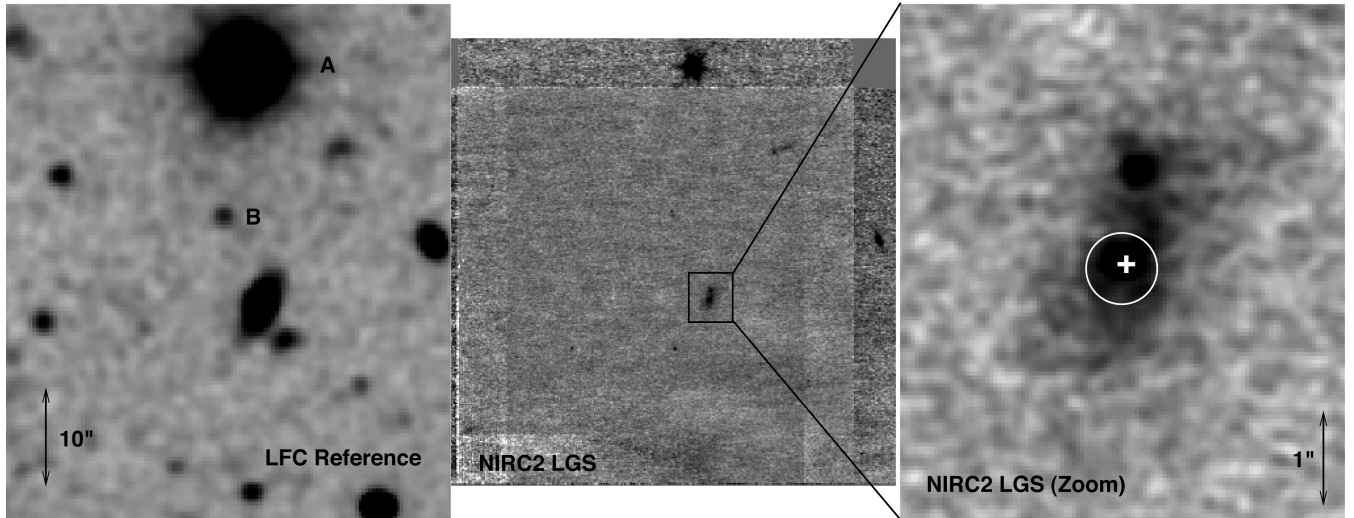
**Figure 2.** PTF10iya astrometry. The left-hand panel displays the Palomar LFC $r'$ reference imaging of the field of PTF10iya. Due to the relative sparseness of the field, the image contains only two point sources in common with the NIRC2/LGS imaging (middle panel), marked 'A' and 'B'. Using only these two sources, we calculate the 99.7 per cent containment radius for PTF10iya to be 350 mas. This localization region is shown in a zoomed-in version of the NIRC2/LGS imaging in the right-hand panel. The position of the nucleus of SDSS J1438, marked with a plus sign, is consistent with the location of the transient emission. The point source to the north-west is ruled out as a counterpart to PTF10iya at large confidence, and the lack of association is further reinforced by the absence of variability of this point source over the course of 6 months. All images are oriented with north up and east to the left.

**Table 3.** Optical spectra of PTF10iya.

| Date[a] (UT) | Telescope/instrument | Wavelength coverage (Å) | Exposure time (s) | Spectral resolution (Å) |
|---|---|---|---|---|
| June 8.43 | Keck I/LRIS (blue) | 3500–5600 | 450.0 | 7.0 |
| June 8.43 | Keck I/LRIS (red) | 5600–10100 | 370.0 | 6.5 |
| June 9.10 | WHT/ISIS (blue) | 3100–5300 | 600.0 | 3.4 |
| June 9.10 | WHT/ISIS (red) | 5300–9500 | 600.0 | 7.3 |
| June 12.49 | Keck I/LRIS (blue) | 3500–5600 | 600.0 | 4.0 |
| June 12.49 | Keck I/LRIS (red) | 5600–10100 | 600.0 | 6.5 |
| July 8.29 | Keck I/LRIS (blue) | 3500–5600 | 1200.0 | 4.0 |
| July 8.29 | Keck I/LRIS (red) | 5600–10100 | 1200.0 | 6.5 |

[a] UT at the beginning of exposure.

were combined into a single co-add using the SWARP software package.[6] The resulting stacked image is shown in the left-hand panel of Fig. 2.

## 2.6 Optical spectroscopy

We undertook a series of spectroscopic observations of PTF10iya with the Intermediate dispersion Spectrograph and Imaging System (ISIS) mounted on the 4.2-m William Herschel Telescope (WHT; June 9) and the Low Resolution Imaging Spectrometer (LRIS; Oke et al. 1995) mounted on the 10-m Keck I telescope (June 8, June 12, July 7). For all spectra, the slit was oriented at the parallactic angle to minimize losses due to atmospheric dispersion (Filippenko 1982). Details of the observational setup for each respective spectrum are provided in Table 3.

All spectra were reduced using standard routines (see e.g. Ellis et al. 2008 for details). Spectra were extracted optimally (Horne 1986) within the IRAF environment. A dispersion solution was computed using afternoon calibration spectra of arc lamps, and then adjusted for each individual exposure using night-sky

lines. Telluric atmospheric absorption features were removed using the continuum from spectrophotometric standard stars (Wade & Horne 1988; Matheson et al. 2000). Finally, a sensitivity function was applied using observations of spectrophotometric standards at a comparable airmass. The red and blue arms were rebinned to a common dispersion and then joined across the dichroic.

To account for slit losses, we have adjusted the flux calibration for all four spectra using broad-band photometry from our (unsubtracted) P60 images at comparable epochs. Three of the resulting spectra are shown in Fig. 3.

## 2.7 Radio observations

We observed the location of PTF10iya with the NRAO[7] Expanded Very Large Array (EVLA) for 1 h on 2011 April 29.3 UT. Observations with a total bandwidth of 256 MHz were obtained at centre frequencies of 1.3 and 8.4 GHz. A compact source (J1426+3625)

---

[6] See http://www.astromatic.net/software/swarp.

[7] The National Radio Astronomy Observatory (NRAO) is a facility of the National Science Foundation operated under cooperative agreement by Associated Universities, Inc.
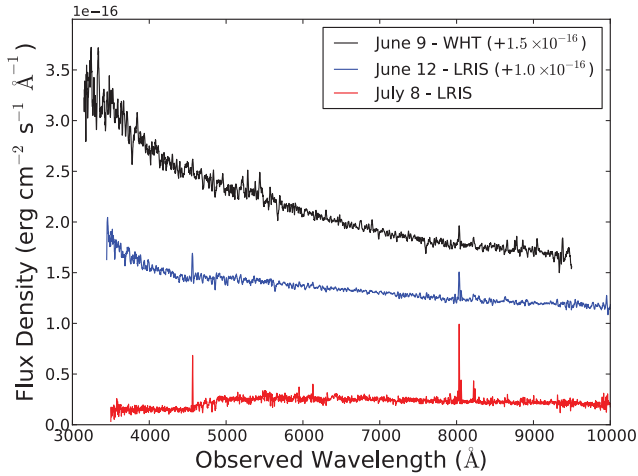
**Figure 3.** Spectroscopic observations of PTF10iya/SDSS J1438. The spectra from June 9 (WHT) and June 12 (LRIS) have been offset for clarity. Our spectrum from June 8 obtained with LRIS is not plotted, as it is nearly identical to the WHT spectrum.

near PTF10iya was observed every 4–6 min for accurate phase calibration, while 3C 286 was observed at the end of the run for the bandpass and flux-density calibration. The data were reduced and imaged using the AIPS (Astronomical Image Processing System) software package.

There was no emission detected at the position of PTF10iya to $3\sigma$ limits of 0.13 and 0.07 mJy at 1.3 and 8.4 GHz, respectively. At the distance of the host galaxy (Section 3.3), this corresponds to spectral luminosities of $<1.4 \times 10^{29} \, \text{erg s}^{-1} \, \text{Hz}^{-1}$ (1.3 GHz) and $<7.8 \times 10^{28} \, \text{erg s}^{-1} \, \text{Hz}^{-1}$ (8.4 GHz).

### 2.8 Additional archival data

As discussed in Section 2.1, PTF10iya is spatially coincident (see Section 3.1 for a detailed discussion of astrometry) with the extended source SDSS J1438. The photometry (model magnitudes) provided by SDSS implies a modestly red galaxy ($g' - r' = 0.72$ mag).

The location of PTF10iya was observed with the Very Large Array (VLA) at 1.4 GHz in 1995 December as part of the Faint Images of the Radio Sky at Twenty centimetres (FIRST; Becker, White & Helfand 1995). No source is detected at this location to a $3\sigma$ limiting flux density of 0.39 mJy. There is no source consistent with the location of PTF10iya in either the *Fermi* Large Area Telescope (LAT; 100 MeV–100 GeV) 1-year Point Source Catalogue (Abdo et al. 2010) or the ROSAT (0.1–2.4 keV) All-Sky Survey Bright Source Catalogue (Voges et al. 1999).

### 3 ANALYSIS

### 3.1 Astrometry

We first determine if there is any discernible offset between the observed transient emission and the nucleus of the galaxy SDSS J1438, as this greatly constrains viable models for the outburst. Because of the significantly smaller pixel scale (0.38 arcsec, compared with 1.0 arcsec for the P48 camera), we initially consider the P60 imaging.

Starting with the $g'$ data (where the transient emission is detected most strongly), we compute an astrometric solution for the refer-

ence image using 20 point sources in SDSS. The $1\sigma$ uncertainty associated with the absolute astrometric calibration is 90 mas in each coordinate. Using the centroiding method from SEXTRACTOR,[8] we measure a position for SDSS J1438 in our reference images of $\alpha = 14^h38^m40^s.988$, $\delta = +37°39'33''.43$ (J2000.0), consistent within the stated uncertainties with the SDSS measurement.

Aligning our P60 $g'$ image from 2010 June 7 with the co-added P60 reference image using 15 common point sources, we measure a dispersion of 0.20 pixel (80 mas) in each direction. On the subtracted image, we measure a position for the transient emission of $\alpha = 14^h38^m40^s.983$, $\delta = +37°39'33''.46$, corresponding to an offset from SDSS J1438 of $(+0.09, -0.14)$ pixels. Repeating the process for the $r'$ and $i'$ filters yields similar results. Thus, based solely on the P60 observations, we conclude that PTF10iya occurred within 120 mas (radius) of the nucleus of SDSS J1438 (68 per cent confidence interval). At $z = 0.224$ (Section 3.3), this corresponds to a projected distance of $d < 420$ pc.

The significantly improved angular resolution provided by the LGS/AO imaging system with NIRC2 could provide even tighter constraints on any offset between PTF10iya and SDSS J1438. It is clear from the LGS image (Fig. 2, right-hand panel) that a point source is detected offset from the nucleus of SDSS J1438: using the NIRC2 (wide-camera) pixel scale (0.039686 arcsec), we measure a radial offset of 970 mas (corresponding to a cardinal offset of 140 mas west, 960 mas north at the specified position angle of $0°$).

Aligning the NIRC2 data from 2010 June 18 with optical imaging of the field is complicated by the lack of sources common to both frames. Even in our deepest LFC stack, we find only two point sources[9] present in both images (Fig. 2, sources 'A' and 'B'). We therefore allow for only a translational offset (i.e. $\Delta x$, $\Delta y$) between the two images. In other words, we have fixed the relative scale and rotation (based on the known NIRC2 pixel scale and position angle), and calculated the average shift between the two point sources. The resulting uncertainty associated with this procedure, calculated as the average offset between the positions of sources A and B in the LFC and NIRC2 images, is 50 mas in each coordinate.

Using the resulting astrometry, we measure a position for the point source of $\alpha = 14^h38^m40^s.968$, $\delta = +37°39'34''.43$. Thus, the point source is offset from the transient location by 990 mas in radius. Even if we assume a relatively conservative uncertainty of 100 mas in each coordinate (double the derived value) to account for the lack of common sources for registration, we still conclude that the point source is offset from PTF10iya with overwhelming confidence.

On the other hand, in the NIRC2 image we measure a position for SDSS J1438 of $\alpha = 14^h38^m40^s.980$, $\delta = +37°39'33''.47$. This falls only 40 mas from the location of PTF10iya, fully consistent within the errors. This is clearly illustrated in the right-hand panel of Fig. 2, where the centroid of SDSS J1438 (indicated with a plus sign) falls within the 99.7 per cent confidence (350 mas adopting our conservative estimate) localization of PTF10iya. The point source, however, is well outside this position.

Two additional lines of evidence further argue against an association between the offset NIR point source and the optical transient PTF10iya. Using the $K$-band magnitude for the nearby bright star 2MASS J143841.12+3739571 (source A in Fig. 2) from the

---

[8] See http://www.astromatic.net/software/sextractor.
[9] The requirement that the common sources be unresolved by default precludes the usage of SDSS J1438.
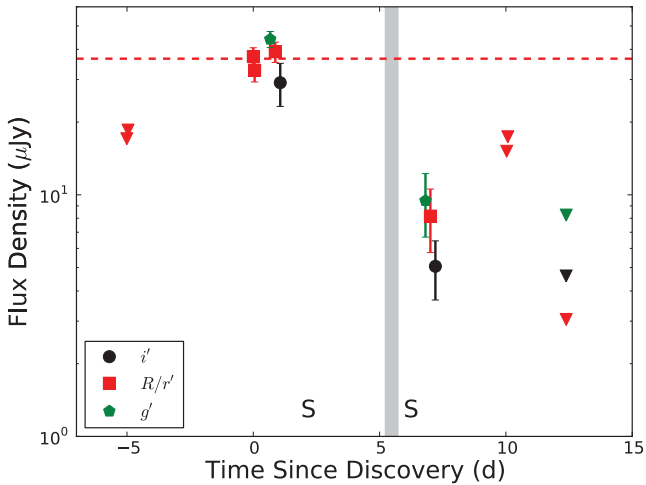
**Figure 4.** Observed optical light curve of PTF10iya, around the time of outburst. The time is referenced to the P48 discovery on June 6.302. The inverted triangles represent $3\sigma$ upper limits. The shaded grey vertical bar indicates the epoch of our *Swift* X-ray and UV observations. The horizontal dashed line indicates the quiescent ($r'$) magnitude of the host galaxy SDSS J1438. The times of optical spectroscopic observations are marked with an 'S'. No correction has been applied for extinction within the host galaxy (Section 3.3). Note that the $i'$- and $g'$-band data have been offset slightly in the horizontal direction for plotting purposes.

Two-Micron All-Sky Survey Point Source Catalog (Skrutskie et al. 2006) as a reference, we measure a magnitude of $K = 19.61 \pm 0.08$ (Vega) for the offset point source on 2010 June 18. Within uncertainties, this value remains constant in our next epoch of $K$-band imaging nearly 6 months later. In addition, in terms of flux density ($f_\nu$), the point source is actually brighter than the contemporaneous optical limits from P60. Given that the observed spectrum of PTF10iya was extremely blue (Section 3.2), it seems even more unlikely that this point source is associated with PTF10iya.

As the offset NIR point source is undetected in even our deepest (P200) optical imaging of the field, the object could either be a foreground cool dwarf star, or an unresolved overdensity in SDSS J1438.[10] We shall assume it is unrelated to PTF10iya for the remainder of this work.

To summarize, we conclude that the location of the transient PTF10iya is consistent with the nucleus of the galaxy SDSS J1438. Our 99.7 per cent confidence localization, with a radius of 350 mas, corresponds to a projected distance of 1.2 kpc at $z = 0.224$ (the 68 per cent confidence radius of 150 mas corresponds to a projected distance of only 540 pc). Given the astrometric alignment, together with the detection of absorption features in the transient spectra (Section 3.2), we shall assume for the remainder of this work that PTF10iya is associated with SDSS J1438.

### 3.2 Light curve, spectral energy distribution and energetics

The optical light curve of PTF10iya (i.e. after subtracting host-galaxy contamination) is shown in Fig. 4. Given the non-detection with P48 on June 1, we can place a limit on the rise time of $\tau_r < 5$ d ($\mathrm{d}m/\mathrm{d}t > 0.15$ mag d$^{-1}$). The $R/r'$ flux remains roughly constant

[10] While M dwarfs are known to undergo dramatic, blue outbursts and can sometimes be confused for extragalactic transients (e.g. Kulkarni & Rau 2006), the time-scale of PTF10iya is orders of magnitude longer than any known such outburst.

for at least 1 day, after which it declines quite steeply at a rate of $\gtrsim 0.3$ mag d$^{-1}$, or an e-folding time-scale of $\tau_d \approx 4$ d. A similar decay is seen in both the $g'$ and the $i'$ filters.

Our detections of PTF10iya are largely clustered into two distinct epochs: June 6–9 (P48 and P60 optical photometry, WHT and LRIS optical spectroscopy) and June 11–13 (P60 optical photometry, *Swift* UV and X-ray photometry, and LRIS spectroscopy). With only limited constraints on the light-curve evolution, we assume that the flux in all bandpasses is approximately constant over the course of each of the two epochs, and proceed to study the broad-band SED.

In order to do so, we must (1) remove the contribution of the host galaxy SDSS J1438 from our spectroscopic observations; and (2) deredden the (subtracted) spectra and photometry to account for extinction within the host galaxy. As described in Section 2.6, the absolute flux scale for each spectrum has been calculated using contemporaneous P60 photometry of the host plus transient (i.e. before the image-subtraction process). To remove the host-galaxy contribution from our June spectra of PTF10iya, we thus subtracted the observed LRIS spectrum from July 7 (which is dominated by host light).

While the initial spectra contained both emission and absorption lines consistent with the redshift of SDSS J1438, the resulting subtracted spectra are largely featureless with a relatively strong blue continuum (Fig. 5). All residual features are narrow and correspond to nebular emission or stellar absorption lines seen in the late-time host spectrum, and thus could result from small mismatches in resolution, slit orientation or wavelength solution.

To account for host-galaxy extinction, we use the reddening law inferred for starburst galaxies from Calzetti (2001) with $E(B - V)_{\mathrm{gas}} = 0.40$ mag, which we derive from the observed Balmer decrement (Section 3.3). We discuss the effect of uncertainties in the inferred extinction on our results in what follows.

In Fig. 5, we plot the derived host- and extinction-corrected UV/optical SED of PTF10iya at both epochs. The broad-band photometry and spectra agree reasonably well and suggest that any systematic uncertainties introduced in this process are relatively modest.

We consider several continuum models in attempting to fit the observed UV/optical SEDs. A power-law model ($f_\lambda \propto \lambda^{-\alpha}$) fails to reproduce the observed spectral curvature (particularly for the June 6–9 data; left-hand panel of Fig. 5), and significantly overpredicts the UV flux. A blackbody spectrum, however, provides a reasonable description of the data at both epochs. The best-fitting blackbody models are plotted in Fig. 5, while the derived fit parameters are displayed in Table 4 .

Two sources of uncertainty could potentially introduce large systematic errors into these results. First, improper flux calibration (particularly in the near-UV, where atmospheric absorption can be highly variable) or host-galaxy subtraction could bias the derived blackbody parameters. Our nearly simultaneous LRIS (June 8.43) and WHT (June 9.10) spectra allow us to test this to some extent, as the spectrum is unlikely to have evolved dramatically over this

**Table 4.** Optical/UV blackbody SED fit parameters.

| Dates | $E(B - V)_{\mathrm{gas}}$ (mag) | $T$ ($10^4$ K) | $L_{\mathrm{BB}}$ ($10^{44}$ erg s$^{-1}$) | $R_{\mathrm{BB}}$ (au) |
|---|---|---|---|---|
| June 6–9 | 0.40 | $2.1 \pm 0.3$ | $4.8 \pm 1.4$ | $130 \pm 20$ |
| June 6–9 | 0 | $1.3 \pm 0.2$ | $0.8 \pm 0.2$ | $140 \pm 30$ |
| June 11–13 | 0.40 | $2.2 \pm 0.3$ | $1.4 \pm 0.3$ | $63 \pm 13$ |
| June 11–13 | 0 | $1.5 \pm 0.2$ | $0.27 \pm 0.09$ | $57 \pm 12$ |
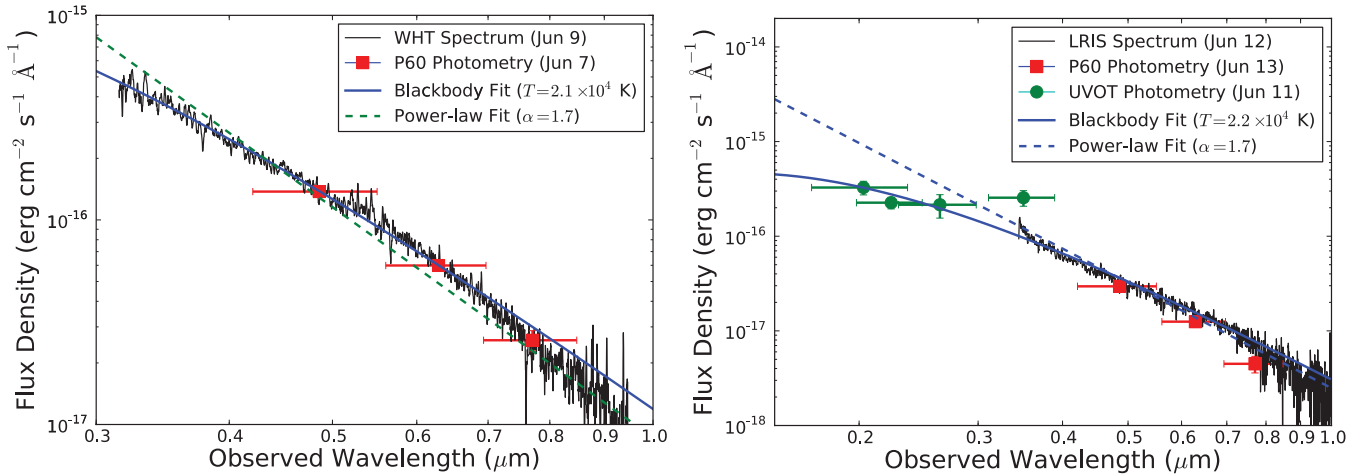
**Figure 5.** Host-galaxy-subtracted and extinction-corrected SED of PTF10iya. Left-hand panel: the June 9 WHT spectrum, with P60 (host-subtracted) photometry overlaid. A blackbody fit results in a temperature of $T_1 = 2.1 \times 10^4$ K. The power-law model (dashed line) does not reproduce the observed curvature in the spectrum as well as a Planck function. Right-hand panel: the June 12 LRIS spectrum. Also overlaid are host-subtracted optical photometry from P60 and UV photometry from *Swift*/UVOT. The best-fitting blackbody function, with $T_2 = 2.2 \times 10^4$ K, is plotted as a solid line. The fit quality is not as high as the previous epoch, but the Planck function better reproduces the turnover in the SED bluewards of 3000 Å than a simple power-law fit (dashed line).

period. We find similar fit parameters for both spectra, although the spread is significantly larger than the formal error from a single fit. We therefore adopt the difference in the derived fit parameters between two spectra as our estimated uncertainty for the June 6–9 epoch. A comparable fractional uncertainty is applied to the data from June 11 to 13, where only a single spectrum is available.

Secondly, because the optical bandpass falls on the Rayleigh–Jeans tail, small changes to the extinction correction (either the magnitude or the dependence with wavelength) could significantly impact the derived fit parameters. Most importantly, minor changes in the UV flux and derived temperature could dramatically affect the derived blackbody luminosity, as $L_{BB} \propto T^4$. We therefore repeat the above analysis, fitting blackbody spectra to the uncorrected SEDs [i.e. $E(B - V) = 0$ mag], and treat these results as lower limits on the blackbody luminosity and temperature. The results of this analysis are shown in Table 4.

Independent of the details of the extinction correction, we conclude that the UV/optical SED of PTF10iya is reasonably well fitted by a blackbody spectrum with temperatures of the order of a few times $10^4$ K. The temperature does not vary dramatically over the course of our observations (June 6–13), though the luminosity does decrease by a factor of 3–4. Likewise, the blackbody radius appears to decrease during this period, although this result is not particularly significant.

In Fig. 6, we plot the broad-band (optical, UV and X-ray) extinction-corrected SED of PTF10iya, this time in terms of $\nu L_\nu$. The best-fitting UV/optical blackbody, with $T = 2 \times 10^4$ K, significantly underpredicts the X-ray flux. While it is possible to fit the optical and X-ray data with a single blackbody with $T \approx 6 \times 10^5$ K (dashed cyan line), the fit is incompatible with the range of possible X-ray spectral indices (blue shaded region), and severely overpredicts the UV flux. We conclude that the X-ray emission is produced by a physical process distinct from that of the observed UV/optical emission.

In terms of $\nu L_\nu$, PTF10iya emitted a comparable amount of energy in the X-rays as in the UV/optical bandpass. Over the range 0.3–10 keV, we find $L_X = 1 \times 10^{44}$ erg s$^{-1}$, about one to three times the UV/optical blackbody luminosity at this time (depending on the extinction correction). To estimate the total energy radiated, we mul-
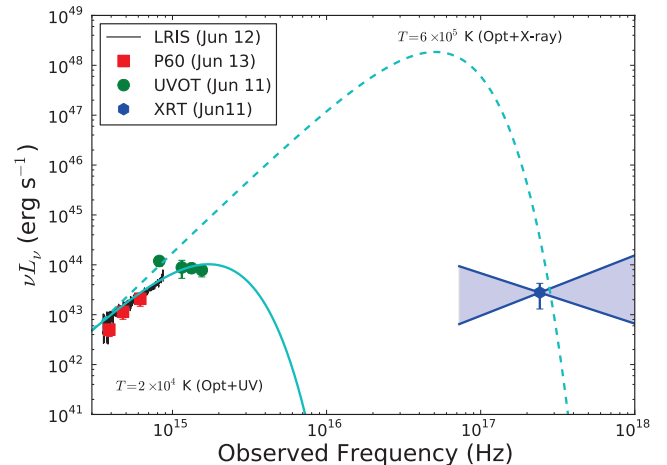


**Figure 6.** Broad-band SED of PTF10iya. We have plotted the LRIS spectrum from June 12, P60 photometry from June 13, and UVOT and XRT photometry from June 11. A blackbody fit to incorporate both the optical and X-ray data requires $T \approx 6 \times 10^5$ K, but is inconsistent with the observed X-ray spectrum (the range of allowed power-law indices is indicated by the shaded blue region) and severely overpredicts the UV flux. On the other hand, a blackbody fitting both the UV flux and the optical flux ($T = 2 \times 10^4$ K) cannot account for the bright X-ray emission.

tiply the mean blackbody luminosity by an approximate duration of 10 d, and find $E_{rad} \approx 3 \times 10^{50}$ erg.

### 3.3 Host galaxy

The July 8 spectrum of SDSS J1438, after dereddening (see below), is plotted in Fig. 7. The spectrum is clearly a composite, containing both absorption features from an underlying stellar population and a series of narrow nebular emission lines. In particular, we detect Ca II H&K, as well as H$\delta$, H$\epsilon$, H$\zeta$, H$\eta$, H$\theta$, H$\iota$ and H$\kappa$, all resolved in absorption. Likewise, typical galaxy emission features, including [O II] λ3727, H$\beta$, [O III] λ5007, [N II] λ6548, H$\alpha$, [N II] λ6584 and [S II] λλ6716, 6731, are all clearly detected from SDSS J1438. Using
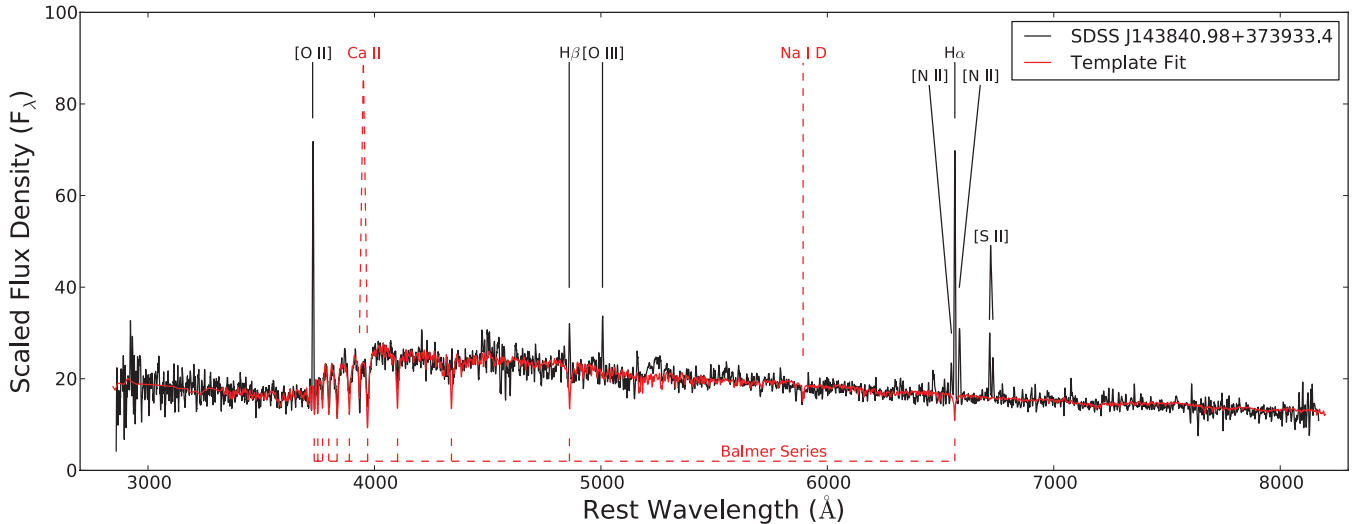
**Figure 7.** De-redshifted ($z = 0.224\,05$) and extinction-corrected [$E(B - V)_{\text{gas}} = 0.40$ mag] host-galaxy spectrum (black) and template fit (red). Following Tremonti et al. (2004), we fit a linear combination of 39 stellar synthesis templates from Bruzual & Charlot (2003) in order to remove the stellar continuum from the spectrum of SDSS J1438. The resulting emission-line intensity ratios (Fig. 8) were then calculated using the subtracted spectrum.

the strongest unblended emission lines, we measure a redshift of $z = 0.224\,05 \pm 0.000\,06$. All of the emission lines are unresolved by the red arm of our LRIS spectrum, with a full width at half-maximum intensity (FWHM) of $\sim$6.5 Å.

We can estimate the extinction along the line of sight to the source using the observed intensity ratios of host-galaxy Balmer emission lines. Fitting a Gaussian profile to the lines, we find that $(L_{\text{H}\alpha}/L_{\text{H}\beta})_{\text{obs}} = 4.4 \pm 0.4$. Assuming Case B recombination (Osterbrock 1989) and the relation from Calzetti (2001), we find $E(B - V)_{\text{gas}} = 0.40 \pm 0.08$ mag.

The fundamental issue we wish to resolve is the origin of these emission lines. The atoms could be ionized by the hard power-law spectrum generated by gas accretion on to a central SMBH (i.e. an AGN), UV photons from young, massive O and B stars (i.e. star formation), or as part of a phenomenon known as a low-ionization nuclear emission-line region (LINER; Heckman 1980), which are likely related to AGNs, possibly resulting from changes to the geometry of the disc at low accretion levels (e.g. Ho 2008).

Typically this is done via a diagnostic diagram (Baldwin, Phillips & Terlevich 1981; Veilleux & Osterbrock 1987) which compares various emission-line intensity ratios. In order to extract the line flux due to the central source, however, we must first remove any contributions from the underlying stellar population (in particular, Balmer-series absorption; e.g. Ho, Filippenko & Sargent 1997). Following Tremonti et al. (2004) and Kauffmann et al. (2003b), we fit a version of the dereddened host spectrum with the emission lines removed to a linear combination of a series of 39 template spectra constructed from the stellar synthesis models of Bruzual & Charlot (2003). The resulting least-squares fit (restricting the weighting coefficients to be positive) is shown in red in Fig. 7, and does a reasonable job reproducing the observed host spectrum across the entire bandpass.

After subtracting the template to remove stellar contamination, we measure the following diagnostic ratios: $L_{\text{[O III]}\lambda5009}/L_{\text{H}\beta} = 0.65 \pm 0.07$, $L_{\text{[N II]}\lambda6583}/L_{\text{H}\alpha} = 0.29 \pm 0.04$, $L_{\text{[S II]}\lambda\lambda6716,6731}/L_{\text{H}\alpha} = 0.38 \pm 0.05$ and $L_{\text{[O I]}\lambda6300}/L_{\text{H}\alpha} < 0.03$. The resulting diagnostic diagrams, including division lines between star-forming galaxies, AGNs and LINERs from Kauffmann et al. (2003b), Kewley & Dopita (2002) and Ho et al. (1997), are shown in Fig. 8. Also

plotted are analogous measurements for a large number of galaxy spectra from the MPA/JHU value-added SDSS catalogue.[11]

In all three plots, SDSS J1438 falls firmly within the locus of star-forming galaxies from SDSS. There may be a slight excess of [S II] $\lambda\lambda$6716, 6731 relative to H$\alpha$, as the host lies directly on the dividing line between star-forming galaxies and LINERs from Ho et al. (1997). However, even on this plot, SDSS J1438 appears to be more consistent with the star-forming galaxies from SDSS than the LINER branch, and does not reach the theoretical limit from Kewley & Dopita (2002). The simplest interpretation, then, is that the narrow emission lines in SDSS J1438 result from photoionization by the UV photons copiously produced by young, massive stars.

The observed morphology of SDSS J1438 further reinforces the notion that this galaxy either is or recently was actively forming new stars. Using the GALFIT software (Peng et al. 2002), we fit the $r'$ LFC images of SDSS J1438 to a Sérsic profile (Sérsic & Pastoriza 1967), allowing the concentration parameter ($n$) and the effective radius ($r_{\text{e}}$) to vary freely. We find that a good fit (both in terms of $\chi^2$ per d.o.f. and by visual inspection) is achieved when $n \approx 0.65$ and $r_{\text{e}} \approx 1.7$ arcsec. Analogous fits to the SDSS $g'$ and $r'$ images yield similar results.

The relatively small concentration number suggests that the emission from SDSS J1438 is dominated by a disc-like profile; for bulge-dominated systems, the radial profile is typically well fitted by a de Vaucouleurs function ($n = 4$). Adding a bulge profile ($n = 4$) significantly reduces the fit quality. By varying the fit parameters and examining the residuals, we estimate that the ratio of the bulge luminosity to total luminosity ($L_{\text{B}}/L_{\text{T}}$) is $\lesssim$30 per cent, a typical value for spiral galaxies.

With this (approximate) deconvolution, we can constrain the mass of the central SMBH using the observed bulge luminosity versus black hole mass relation (Magorrian et al. 1998). Integrating our (dereddened) spectrum of SDSS J1438 over the rest-frame $V$ band, we find $M_V = -20.75 \pm 0.15$ mag ($M_V = -19.82 \pm 0.17$ mag neglecting any host extinction). Applying the bulge

---

[11] See http://www.mpa-garching.mpg.de/SDSS.
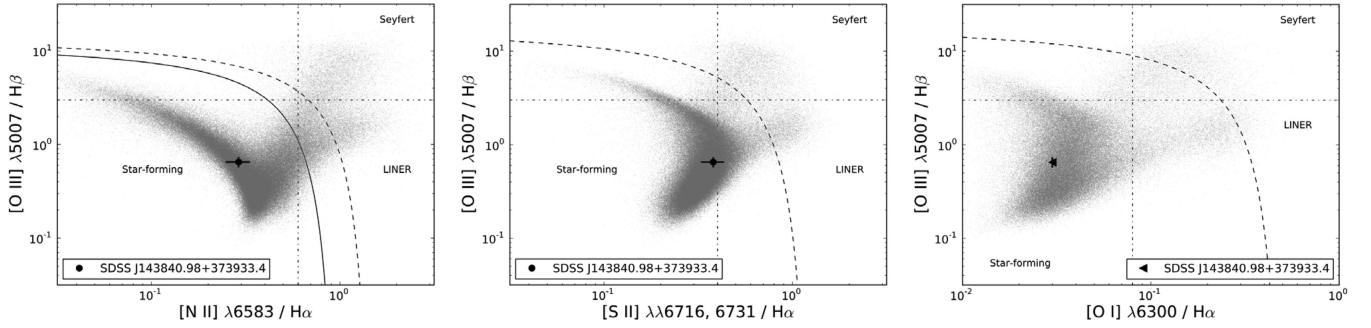
**Figure 8.** Diagnostic emission-line diagrams for SDSS J1438. The empirical dividing line between star-forming and active galaxies from Kauffmann et al. (2003b) is shown as the solid line in the left-hand panel, while analogous dividing lines from Ho et al. (1997) are indicated with the dot–dashed lines. The theoretical dividing line from Kewley & Dopita (2002) is plotted as a dashed line. Analogous measurements for SDSS galaxy from the MPA-JHU value-added catalogue are shown as the grey dots.

luminosity-to-total luminosity correction from above ($L_B/L_T \lesssim 0.3$) and using the relation from Lauer et al. (2007), we find $\log(M_{BH}/M_\odot) \lesssim 7.5$ [$\log(M_{BH}/M_\odot) \lesssim 7.0$, neglecting any host-galaxy extinction correction], suggesting a similar mass black hole to that found in the centre of the Milky Way ($M_{BH} \approx 4 \times 10^6 \, M_\odot$; Ghez et al. 2008).

Finally, we can use the results of our template fitting to infer additional global properties of the galaxy SDSS J1438. Following Kauffmann et al. (2003a), we calculate the strength of the 4000 Å break [$D_n(4000) = 1.2 \pm 0.1$] and the equivalent width (EW) of the H$\delta$ absorption feature [EW(H$\delta$) = $3.9 \pm 1.0$ Å]. The ratio of $D_n(4000)$ to EW(H$\delta$) indicates that SDSS J1438 has been undergoing relatively continuous star formation over its history (see fig. 3 from Kauffmann et al. 2003a). However, the relatively strong H$\delta$ feature suggests a significant contribution from A-type stars, and we infer that the bulk of star formation likely ended within the last 0.1–1 Gyr. The current star formation rate, derived from the extinction-corrected luminosity in H$\alpha$, is $1.5 \pm 0.5 \, M_\odot \, yr^{-1}$ (using the calibration from Kennicutt 1998).

We can further utilize the derived 4000 Å break strength and H$\delta$ EW to estimate the mass-to-light ratio ($M/L$) in SDSS J1438. Using the models from Kauffmann et al. (2003a), we find $-0.4 \lesssim \log(M/L) \lesssim -0.1$. We thus infer a total stellar mass of $M \approx 10^{10} \, M_\odot$ from our extinction-corrected spectrum.

# 4 INTERPRETATION

Having completed our analysis of the available data (Section 3), we now turn our attention to interpretation. Ultimately, we wish to understand the physical processes responsible for the observed transient emission from PTF10iya. Given the extreme luminosity and short-lived duration, here we consider four potential origins for PTF10iya: the afterglow of a gamma-ray burst (GRB; Section 4.1), a core-collapse SN (Section 4.2), gas accretion on to a central SMBH (AGN or LINER; Section 4.3), and the tidal disruption of a star by an (otherwise quiescent) SMBH (Section 4.4).

## 4.1 Gamma-ray burst afterglow

For their brief durations, GRBs are the most luminous transients in the Universe, reaching peak optical absolute magnitudes as large as $M_V \approx -37$ mag (GRB 080319B; Racusin et al. 2008; Bloom et al. 2009) and X-ray luminosities well in excess of $10^{44} \, erg \, s^{-1}$ (e.g. Evans et al. 2007). However, GRB afterglow emission, widely believed to result from synchrotron radiation from electrons accel-

erated by an outgoing relativistic blast wave (see e.g. Piran 2005), is a distinctly *non-thermal* process. The SED in the optical regime is typically well described by a power law ($f_\nu \propto \nu^{-\beta}$) with $\beta \approx 0.5$ to 1.5 (i.e. $f_\nu$ increases at longer wavelengths; Sari, Piran & Narayan 1998). Extinction in the host galaxy only serves to make the observed spectrum even redder. This contrasts sharply with the observed UV/optical emission from PTF10iya. Even if the SED of PTF10iya does not match a blackbody, it is much too blue to be compatible with a GRB afterglow.

## 4.2 Supernova

Like GRB afterglows, core-collapse SNe are capable of generating bright, transient X-ray (e.g. $L_X = 6 \times 10^{43} \, erg \, s^{-1}$; Soderberg et al. 2008; Modjaz et al. 2009) and optical (e.g. $M = -22.7$ mag; Quimby et al. 2007) emission. Furthermore, the spectra of young core-collapse SNe are typically dominated by a blue, thermal continuum.

However, PTF10iya is unlikely to have resulted from any known class of SN. To begin with, the derived blackbody radius ($\sim$300 au) is much larger than the radius of a typical stellar progenitor, and the outgoing ejecta would not have time to reach such a large distance travelling at typical SN velocities. Furthermore, all known X-ray SNe are at least two orders of magnitude fainter than PTF10iya.[12] The X-ray emission from core-collapse SNe typically results from shock heating of a moderately dense circumstellar medium (e.g. Immler & Lewin 2003). It is therefore quite long-lived, in some cases for decades. Moreover, the optical spectra of such SNe generally exhibit narrow and intermediate-width emission lines (e.g. Smith et al. 2010).

Finally, we note that the decay time-scale observed in the optical ($\sim$0.3 mag d$^{-1}$) is shorter than that of any previously observed SNe thought to be powered by radioactive decay.[13] The current record holders are SN 2010X (Kasliwal et al. 2010) and SN 2002bj

---

[12] The X-ray emission observed from SN 2008D resulted from the breakout of the shock from the stellar envelope (Colgate 1974). As such, it was quite short-lived (hundreds of seconds), and disappeared entirely as late as 5 d after the detected outburst.

[13] The fast decay rate could result to some extent from spectral evolution (i.e. varying $T_{BB}$), and therefore may not represent the true evolution of the bolometric luminosity. For example, the light curve of PTF 09uj, which is believed to be powered by shock breakout from a dense circumstellar wind, declined even more quickly in the $R$ band ($\sim$3 mag in 25 d; Ofek et al. 2010). We have already, however, dismissed a shock-breakout origin for PTF10iya.

(Poznanski et al. 2010), both decayed after the peak at a rate of $\sim 0.2 \, \mathrm{mag} \, \mathrm{d}^{-1}$. It would require an extremely small ejecta mass and/or an outflow entirely transparent to the gamma-rays produced by the radioactive decay to produce a SN that decayed at such a rapid rate, both of which are inconsistent with the large observed luminosity.

### 4.3 AGN/LINER

The nuclear location of PTF10iya, together with the observed spectrum (reminiscent of the 'big blue bump'; Sanders et al. 1989; Bregman 1990), naturally leads us to consider accretion on to a SMBH as a possible origin (Shields 1978; Malkan & Sargent 1982). Here we determine if gas accretion (either in the form of a normal AGN or a LINER) is consistent with the observed properties of PTF10iya.

To begin with, we must confront the fact that the nebular emission lines in the spectrum of SDSS J1438 do not appear to be caused by AGN photoionization, even with a low-ionization parameter as in a LINER. In and of itself, however, this is not sufficient to entirely discount continuous accretion activity. Because of the non-zero size of our slit, our spectrum of the 'nucleus' of SDSS J1438 could be contaminated by nearby H II regions. For example, *Hubble Space Telescope (HST)* spectroscopy of NGC 5905, initially classified as a starburst galaxy in a similar analysis to that conducted in Section 3.3, revealed a faint Seyfert nucleus that had previously gone undetected (Gezari et al. 2003).

If we set aside for the moment the nebular emission-line classification, we still must simultaneously account for the short time-scale and the order of magnitude increase in the UV/optical and X-ray flux. The most dramatically variable class of AGNs are the blazars, which are thought to arise when a relativistic jet fed by accretion is oriented directly along our line of sight (e.g. Blandford & Rees 1978; Urry & Padovani 1995). For example, 3C 279 has varied across the entire electromagnetic spectrum by factors of the order of a few on time-scales shorter than days (e.g. Wehrle et al. 1998).

Blazars are typically hosted in massive ($\gtrsim 10^{10} \, \mathrm{M}_\odot$) elliptical galaxies, though individual counterexamples are known (see e.g. Gal-Yam et al. 2002, for a blazar initially thought to be an orphan GRB afterglow). More importantly, blazars are almost exclusively bright radio sources, even in quiescence. Using our post-outburst radio limits from the EVLA (Section 2.7), we calculate an upper limit on the quiescent radio luminosity ($\nu L_\nu$) of $<3 \times 10^{38} \, \mathrm{erg} \, \mathrm{s}^{-1}$ at $\nu = 1.3 \, \mathrm{GHz}$. Even when comparing with samples of blazars selected based on X-ray variability, the ratio of quiescent optical flux to X-ray flux [$\alpha_{OX} \equiv -\log (f_{\nu,O}/f_{\nu,X})/\log (\nu_O/\nu_X) > 1.6$], like the ratio of quiescent radio flux to optical flux [$\alpha_{RO} \equiv -\log (f_{\nu,R}/f_{\nu,O})/\log (\nu_R/\nu_O) < 0.1$], appears inconsistent with the properties of the known blazar population ($\alpha_{OX} = 0.6$–1.4; $\alpha_{RO} = 0.2$–0.5; Beckmann et al. 2003).

Even during outburst, the characteristic double-peaked blazar SED (e.g. Urry & Padovani 1995; Fossati et al. 1997) does not provide a good match to the observed emission from PTF10iya. Well below the first peak ($\nu L_\nu$) in the broad-band spectrum, blazar SEDs are dominated by non-thermal synchrotron radiation, rising as a power law like $\nu^1$. The SED only becomes shallower near the peak frequency. The observed spectrum of PTF10iya, on the other hand, is quite steep, with $\nu L_\nu \propto \nu^{2.7}$. Furthermore, the SED of lower luminosity blazars typically peaks at higher frequencies than that of higher luminosity sources (e.g. Fossati et al. 1998). Objects with peak frequencies as low as the UV typically have peak $\nu L_\nu \gtrsim 10^{45} \, \mathrm{erg} \, \mathrm{s}^{-1}$, several orders of magnitude brighter than PTF10iya.

In contrast, the faintest blazars compiled in the sample of Fossati et al. (1998), with peak $\nu L_\nu \approx 6 \times 10^{44} \, \mathrm{erg} \, \mathrm{s}^{-1}$ (a factor of several brighter than PTF10iya), peak in the soft X-ray band.

Turning now to Seyfert galaxies, we consider two separate classes of known sources, and compare their variability properties to those of PTF10iya. *ROSAT* detected bright ($L_X \gtrsim 10^{42} \, \mathrm{erg} \, \mathrm{s}^{-1}$) X-ray outbursts from a number of narrow-line Seyfert 1 (NLS1) galaxies as part of the All-Sky Survey (Voges et al. 1999). For instance, the nearby ($z = 0.028$) galaxy WPVS 007 was detected in outburst with $L_X \approx 10^{44} \, \mathrm{erg} \, \mathrm{s}^{-1}$ in 1990 November; 3 years later, the X-ray flux had declined by a factor of 400 (Grupe et al. 1995). While WPVS 007 is the most dramatic example, many other NLS1 galaxies were observed by *ROSAT* to vary by more than an order of magnitude on time-scales as short as days (e.g. McHardy et al. 2004). In some cases, the X-ray flare was followed by variability in the optical spectra, including the appearance of high-ionization iron emission lines (e.g. IC 3599; Brandt, Pounds & Fink 1995; Grupe et al. 1995; Komossa & Bade 1999).

However, several properties of either PTF 10iya (the outburst) or SDSS J1438 (the quiescent host) are inconsistent with the NLS1 interpretation. To begin with, the X-ray spectra of NLS1 galaxies are typically significantly steeper (power-law index $\Gamma \approx 3$–5 compared to $\Gamma_{PTF10iya} = 1.8$) than the observed X-ray outburst from PTF10iya (Grupe et al. 2004). The X-ray spectral slope is actually quite crucial to the interpretation of the NLS1 phenomenon, where the observed variability is thought to arise from changes in the covering fraction of a warm absorbing cloud (Grupe, Leighly & Komossa 2008). In addition, optical spectra of NLS1 galaxies are characterized by (1) relatively narrow Balmer emission lines [FWHM(H$\beta$) $< 2000 \, \mathrm{km} \, \mathrm{s}^{-1}$]; (2) weak [O III] $\lambda 5007$ emission ([O III]/H$\beta < 3$); and (3) strong Fe II emission (Osterbrock & Pogge 1985; Goodrich 1989). For SDSS J1438, the [O III] $\lambda 5007$ emission is indeed quite weak. However, while the H$\alpha$ and H$\beta$ emission lines are clearly narrow, there is in fact no sign of a broad component whatsoever – both H$\beta$ and H$\alpha$ are unresolved in our July LRIS spectrum. Together with the lack of Fe II emission, PTF10iya appears to differ fundamentally from the known properties of NLS1 galaxies, or of normal Seyfert 1 galaxies for that matter.

While a Seyfert 2 galaxy (those lacking any evidence for a broad-line region in the optical) may be easier to hide in the spectrum of the quiescent host galaxy, dramatic continuum variability is not typically observed from these sources. One particularly interesting exception merits mention here: NGC 5905 (Bade, Komossa & Dahlem 1996; Komossa & Bade 1999).

Bright X-ray emission ($L_X = 7 \times 10^{43} \, \mathrm{erg} \, \mathrm{s}^{-1}$) was detected from NGC 5905 in 1990 July by the *ROSAT* all-sky survey. Follow-up observations over the subsequent months and years failed to re-detect the source, implying that the quiescent flux is at least two orders of magnitude fainter than the outburst. Like in the NLS1 galaxies, the X-ray spectrum during outburst was quite soft ($\Gamma \approx 4$–5). However, follow-up optical spectroscopy, both from the ground and with *HST*, failed to reveal any broad component to the Balmer emission lines (Komossa & Bade 1999; Gezari et al. 2003).

A variety of models have been proposed to explain the properties of the NGC 5905 outburst (e.g. Komossa & Bade 1999; Li, Narayan & Menou 2002). In the AGN context, Komossa & Bade (1999) explored the possibility of a variable absorbing cloud along the line of sight. In this warm absorber model, the Seyfert nucleus becomes visible by ionizing the ambient medium, making it transparent to soft X-rays (much like a NLS1). This naturally explains the

relatively steep X-ray spectrum observed in NGC 5905 ($\Gamma \approx 5$), but the presence of a significant dust column is required to hide the broad-line region in the optical.

PTF10iya is more difficult to accommodate in the warm absorber framework, as the observed X-ray spectrum is not particularly steep ($\Gamma = 1.8$), and the observed thermal SED in outburst rules out a large amount of dust (at least at that time). We cannot, however, entirely eliminate geometries whereby the observed outburst results from short-lived changes in obscuration along the line of sight. The lingering ambiguity over the origin of the NGC 5905 outburst (see e.g. Li et al. 2002 for a TDF interpretation) reinforces just how difficult such a task can be.

Finally, we consider the known variability properties of low-luminosity AGNs (i.e. LINERs) to see if they could explain our observations of PTF10iya. It was originally thought LINERs exhibited little to no X-ray variability on short time-scales (e.g. Komossa, Böhringer & Huchra 1999), though more recent studies of Type I LINERs have demonstrated variations of $\sim$30 per cent on time-scales of less than 1 d (Pian et al. 2010). Likewise, recent UV studies have shown variability of the order of 50 per cent in the UV in both Type I and II LINERs, though on longer (months) time-scales (Maoz et al. 2005). In fact, at the time of our X-ray detection of PTF10iya (2010 June 11), the observed optical to X-ray spectral index, $\alpha_{OX} \approx 1.1$, is broadly consistent with the properties of known low-luminosity AGNs (Maoz 2007).

However, if SDSS J1438 does indeed host a faint active nucleus (similar to NGC 5905; Gezari et al. 2003), the emission-line flux from the nucleus must be significantly less than the total integrated value across the slit (in order for the line diagnostics to indicate a pure H II region). If we adopt a limit of <10 per cent on the contribution to the extinction-corrected [O III] line and apply the observed correlation between [O III] flux and $L_X$ for AGNs (Heckman et al. 2005), we infer a quiescent X-ray luminosity of $L_X \lesssim 10^{42}$ erg s$^{-1}$. This value is two orders of magnitude less than the observed flaring state; to the best of our knowledge, such a dramatic outburst has never before been observed in a low-luminosity LINER, though the nature of the variability in these sources is not yet well understood.

To summarize, even if we overlook the lack of evidence for AGN activity in SDSS J1438, the emission-line ratios, the historical light curve, and the dramatic increase in the X-ray flux make PTF10iya unique among known AGN outbursts. Of course, we cannot entirely exclude some previously unobserved mode of variability in the gas accretion process. Nevertheless, given the inadequacy of AGNs in explaining the observed properties of PTF10iya, we also seek an alternative possibility.

## 4.4 Tidal disruption flare

Stars passing too close to a SMBH will be torn apart when tidal forces are stronger than their self-gravity (Frank & Rees 1976; Lacy, Townes & Hollenbach 1982; Rees 1988). In the case of solar-type stars (mass $M_*$, radius $R_*$), this disruption will occur outside the event horizon for SMBHs with $M_{BH} \lesssim 10^8$ M$_\odot$ (Hills 1975). Bound stellar debris is sent off on highly elliptical orbits, and should return to pericentre ($R_p$) at a rate $\dot{M} \propto t^{-5/3}$ (Evans & Kochanek 1989; Phinney 1989; Ayal, Livio & Piran 2000; Lodato, King & Pringle 2009; Ramirez-Ruiz & Rosswog 2009). The resulting accretion on to the SMBH powers an outburst known as a TDF.

In the simplest models, the returning debris shocks and circularizes, forming a torus around the SMBH (e.g. Ulmer 1999; Li et al. 2002). Particularly at late times, the disc should be optically

thick but geometrically thin, and the emergent spectrum should be approximately thermal, with

$$
\begin{aligned}
T &\approx \left( \frac{L_{Edd}}{4\pi R_T^2 \sigma} \right)^{1/4} \\
&= 2 \times 10^5 \left( \frac{M_{BH}}{10^6\,M_\odot} \right)^{1/12} \left( \frac{R_*}{R_\odot} \right)^{-1/2} \left( \frac{M_*}{M_\odot} \right)^{-1/6} \text{K}, \quad (1)
\end{aligned}
$$

where $R_T \approx R_*(M_{BH}/M_*)^{1/3}$ is the tidal radius (where the tidal force due to the SMBH exceeds the self-gravity of the star). As is evident from equation (1), the spectrum peaks in the far-UV, with a large bolometric correction from the rest-frame optical bandpass. For emission from the accretion disc, the bolometric luminosity evolution should approximately follow the mass accretion rate, $L \propto t^{-5/3}$, although the observed flux in a given bandpass could deviate from this behaviour.

It is not surprising, then, that the majority of TDF candidates have been identified through wide-field X-ray (Bade, Komossa & Dahlem 1996; Komossa & Greiner 1999; Greiner et al. 2000; Donley et al. 2002; Esquej et al. 2007, 2008; Maksym, Ulmer & Eracleous 2010) and UV (Renzini et al. 1995; Gezari et al. 2006, 2008, 2009) surveys. PTF10iya differs in important ways from most of these TDF candidates: the derived blackbody temperature of PTF10iya is approximately an order of magnitude smaller than in these sources (which exhibit typical temperatures of a few times $10^5$ K), the decay time-scale is significantly shorter (typical durations of months to years), and, when detected, the X-ray emission is significantly harder (typical power-law indices of $\Gamma \approx 4$–5). Many of these differences could be ascribed to bandpass selection effects, so a more apt comparison would be to the *optically* discovered candidates from van Velzen et al. (2011a). We shall return to this issue shortly.

The blackbody prediction in equation (1) is well motivated at late times, when the fallback rate is sub-Eddington: $\dot{M} \lesssim \dot{M}_{Edd} \equiv L_{Edd}/\epsilon c^2$ ($\epsilon$ is the radiative efficiency of the accretion disc, assumed to be $\sim$0.1). However, for black holes with $M_{BH} \lesssim 3 \times 10^7$ M$_\odot$, the mass accretion rate will *exceed* the Eddington rate for some period of time following disruption. In this case, the accretion disc is likely to be highly advective, and some fraction of the bound material may be blown out from the system as a powerful wind (e.g. King & Pounds 2003; Ohsuga et al. 2005). Strubbe & Quataert (2009) have calculated the expected emission from this super-Eddington outflow, and predict a short-lived ($\Delta t \approx 30$ d), luminous ($L_{peak} \approx 10^{44}$ erg s$^{-1}$) flare with a lower temperature than that seen during the thin-disc phase.

The observed properties of PTF10iya are broadly consistent with the predictions for this super-Eddington phase. The relatively short time-scale, in terms of both the rise and the decline, suggests that the disruption occurred close to the SMBH: $R_p \lesssim 3R_S$, where $R_S$ is the Schwarzschild radius. Likewise, the large bolometric luminosity is consistent with a relatively massive SMBH: $M_{BH} \gtrsim 10^7$ M$_\odot$. For a solar-type star with pericentre distance $R_p \approx 2R_S$ disrupted by a $10^7$-M$_\odot$ black hole, we find $R_{BB} \approx 100$ au, $T_{BB} \approx 10^4$ K and $L_{BB} \approx 10^{45}$ erg s$^{-1}$ a few days after the disruption occurs [taking the fiducial values for the fraction of incoming material expelled in the super-Eddington wind ($f_{out}$) and the terminal wind velocity ($f_v$) from Strubbe & Quataert (2009)]. If we instead allow $f_{out}$ and $f_v$ to vary, we find a range of possible models ($M_{BH} \approx 10^6$–$10^7$ M$_\odot$; $R_p \approx 2R_S - R_T$) can reproduce the observed optical luminosity and colours. With only two epochs of data, however, a detailed test of these models, in particular the temporal evolution, is beyond the scope of this work.

After the accretion rate drops below Eddington, in the tidal disruption model the emission should be dominated by shock-heated material in the accretion disc. Given the predicted temperature for the disc in this phase (equation 1), it is important to check if we would be sensitive to any disc emission in our X-ray and UV observations from 2010 August. Using models for the sub-Eddington disc emission from Strubbe & Quataert (2009) with the system parameters determined above, we estimate $\nu L_\nu(\lambda_{rest} = 2000\,\text{Å}) \lesssim 2 \times 10^{42}\,\text{erg s}^{-1}$. This corresponds to a UVOT $UVW1$ magnitude of $\gtrsim 22.5$. Even neglecting the derived host-galaxy extinction, this value is several magnitudes fainter than our limits at this time. Likewise, the derived X-ray emission from this accretion disc component is well below the upper limits from the XRT at this time.

On the other hand, comparing our late-time ($\Delta t \approx 2$ months) limits with the *observed* UV properties of candidate TDFs from *GALEX* presents a slightly more complex picture. With typical near-UV absolute magnitudes (AB) of $\approx -18$ to $-19$ mag at this time (Gezari et al. 2009), a comparable source would appear with $UVW1 \approx 19.5$–$20.5$ mag at the distance of PTF10iya. One possibility to explain this apparent discrepancy with our derived limits ($UVW1 > 20.5$ mag) is extinction: our derived value of $E(B - V)_{gas} = 0.40$ mag corresponds to $A_{UVW1} \approx 1.5$ mag. With this correction, our 2010 August UVOT limits are not sufficiently deep to rule out UV flares similar to those reported by Gezari et al. (2009). However, our derived extinction correction is quite uncertain. We are therefore left to conclude that our 2010 August *Swift* observations are not sufficiently constraining to either detect or rule out the expected disc signature during the sub-Eddington phase.

A $10^7$-$M_\odot$ SMBH is consistent with the limits for SDSS J1438 derived from the black hole versus bulge luminosity relation (Section 3.3). Furthermore, Strubbe & Quataert (2011) predict that any absorption features in the optical bandpass due to the photoionization of the unbound material should be weaker for more massive black holes, and indeed we do not detect such features in the early-time spectra of PTF10iya. We reiterate, however, that the estimated black hole mass is still sufficiently small to ensure that the disruption would occur outside the event horizon.

In addition to the outburst properties, the host galaxy of PTF10iya is consistent with a TDF interpretation. No variability is seen in the optical light curve in our PTF and Deep Sky imaging of the field in the last few years. The observed emission-line ratios in quiescence indicate a moderately star forming galaxy and are incompatible with photoionization by the hard X-ray continuum common in AGNs. In fact, the host galaxy of PTF10iya, SDSS J1438, bears a strong resemblance to the host galaxy of D23H-1, a candidate TDF discovered by *GALEX* (Gezari et al. 2009). The diagnostic emission-line ratios are all consistent within $2\sigma$ uncertainties, as is the derived line-of-sight extinction.

Several important distinctions between PTF10iya and previous TDF candidates remain, however. First, PTF10iya appears to decay much more rapidly than any previously claimed TDF candidate, even the handful discovered in the optical. Given that the constraints on the outburst dates are much weaker for nearly all previous candidates,[14] this may be simply because PTF10iya was caught shortly after the disruption; the higher cadence of PTF enables detection of short-lived outbursts that might have been missed by other surveys. Nevertheless, the contrast between the two TDF candidates from

van Velzen et al. (2011a), which decayed by $\sim$0.5–1.0 mag in 50 d since discovery, and PTF10iya, which decayed by $\sim$1.5 mag in only 6 d, is quite striking.

Most importantly, the X-ray emission from PTF10iya, which accounts for a significant fraction of the bolometric luminosity, remains a significant challenge for TDF models. Unlike previous TDF candidates discovered in the X-rays, the shallow, non-thermal X-ray spectrum is inconsistent with a simple extrapolation of a $10^5$-K blackbody to high energies.

Recently, two unusual high-energy transients discovered by the *Swift* satellite (Swift J1644+57 and Swift J2058+05) were suggested to result from the tidal disruption process (Bloom et al. 2011a; Burrows et al. 2011; Cenko et al. 2011; Levan et al. 2011; Zauderer et al. 2011). While both sources display extremely luminous ($L_X > 10^{47}\,\text{erg s}^{-1}$) X-ray emission, this was also accompanied by a luminous radio source, with compelling evidence that the outburst marked the birth of a collimated, relativistic outflow (i.e. a jet). One possibility is that the observed emission from PTF10iya is generated by the same process (i.e. tidal disruption), but we are viewing the system from outside the narrow angle of the jet (an 'off-axis' TDF).

Giannios & Metzger (2011) considered off-axis emission from the interaction of a mildly relativistic jet with surrounding material, and predict bright ($L_\nu \gtrsim 10^{30}\,\text{erg s}^{-1}\,\text{Hz}^{-1}$ at 10 GHz), self-absorbed radio emission peaking around a year after disruption.[15] Our radio non-detections (Section 2.7) are an order of magnitude below the predictions of these models, suggesting in this case either that no relativistic jet was generated during the disruption process or that the surrounding environment differed significantly from the nominal parameters assumed by Giannios & Metzger (2011). We note that these limits are significantly more constraining for these radio jet models than previous observations, which were either obtained shortly after disruption (van Velzen et al. 2011a) or solely at low frequency, where self-absorption comes into play (Bower 2011).

If we do not consider relativistic jetted models, we may still be able to explain the observed X-ray flare by analogy with AGNs. Theoretically, for $M_{BH} > 10^7\,\text{M}_\odot$, the density at pericentre is never quite high enough for the gas and radiation to reach thermal equilibrium, and so instead, photons likely Compton upscatter off fast-moving electrons to produce hard X-rays (Strubbe & Quataert 2011). While such a phenomenon, similar to what is observed in the hard X-ray bandpass in AGNs, may account for the X-ray emission from PTF10iya, the process is relatively poorly understood and beyond the scope of this work.

## 5 CONCLUSIONS

To summarize, we reiterate the primary observed properties of PTF10iya:

(i) It was a short-lived ($\tau \approx 10$ d), luminous ($M_{g'} \approx -21$ mag) UV/optical flare.

(ii) After subtracting the host-galaxy contribution, the transient emission is relatively blue, and reasonably well fitted by a blackbody with $T \approx (1\text{–}2) \times 10^4$ K, $R \approx 200$ au and $L \approx 10^{44}\text{–}10^{45}\,\text{erg s}^{-1}$.

(iii) A simultaneous X-ray flare of comparable energy output ($L_X \approx 10^{44}\,\text{erg s}^{-1}$) at $\Delta t \approx 5$ d after the outburst was detected.

---

[14] Two exceptions include D1-9, where a rising light curve was observed in the optical (Gezari et al. 2008), and NGC 5905, where a rising X-ray light curve was observed (Li et al. 2002).

[15] van Velzen, Körding & Falcke (2011b) also consider radio jets from TDFs, but powered instead internally by the accretion process. The predicted radio luminosity and spectra are mostly similar to those of Giannios & Metzger (2011).

(iv) It was astrometrically consistent with the nucleus of a $z = 0.224\,05$ star-forming galaxy with a predominantly disc-like morphology (SDSS J1438).

(v) There is no evidence, either from the historical light curve or host spectrum, for previous episodes of accretion on to the central SMBH, that is, SDSS J1438 does not appear to be an AGN.

After ruling out other known classes of extragalactic variable sources (GRBs and SNe), we have demonstrated that the basic properties of the UV/optical outburst (luminosity, temperature, duration) are broadly consistent with the recent predictions of Strubbe & Quataert (2009) for the early stages following the tidal disruption of a solar-type star by an $\sim 10^7\,M_{\odot}$ SMBH. This picture is further supported by the lack of variability in the historical optical light curve, and the emission-line diagnostic diagrams which suggest an ordinary star-forming galaxy (i.e. not a Seyfert or LINER).

At the same time, PTF10iya differs in important ways from previously identified TDF candidates. While some of this can be understood largely as bandpass biases (e.g. lower blackbody temperature than for UV- and X-ray-selected candidates), the short duration and associated bright X-ray flare suggest a significant diversity if indeed all of these sources do result from the tidal disruption of a star by a SMBH. Without an unambiguous signature, such as the predicted broad (0.01–0.1$c$), blueshifted absorption features in the rest-frame UV bandpass (Strubbe & Quataert 2011), we cannot definitely rule out an unusual AGN outburst scenario.

While much of the interpretation herein has been centred on the TDF framework, it is nonetheless interesting to speculate on what might cause such a short time-scale outburst in an otherwise quiescent AGN. The black hole binary systems known as soft X-ray transients (SXTs) at first glance appear to be potential stellar mass analogues. These systems, such as A0620-00 (Elvis et al. 1975; Gelino, Harrison & Orosz 2001), spend decades in a quiescent state accreting from their companions at extremely low rates ($\dot{M}_{\rm Edd} < 0.01$). After intervals of several decades, however, a thermal viscous instability in the accretion disc triggers a dramatic outburst typically lasting several weeks (e.g. Cannizzo 1993). Since the recurrence time should scale proportionally to black hole mass, a quiescent $10^7$-$M_{\odot}$ black hole would be expected to undergo such an outburst every $\sim 10^6$ yr, much too long to detect on human time-scales. Interpreting AGN outbursts in this manner yields a self-consistent quasar luminosity function (Siemiginowska & Elvis 1997), and can account for the resemblance between the power spectrum of AGNs and stellar mass black hole binaries in the soft/high state (McHardy et al. 2004, 2006).

There are significant problems with this picture, however. First, the thermal viscous instability may not be capable of producing large-amplitude outbursts in SMBH systems, as the gas in these systems is well coupled to the magnetic field even in quiescence due to the larger size of the accretion disc (Menou & Quataert 2001). Even more troubling, the outburst duration should also scale as the black hole mass, so SXT-like outbursts in SMBH systems would have durations of $\sim 10^4$–$10^5$ yr. Conversely, a 10-d outburst in a $10^7$-$M_{\odot}$ system corresponds to an $\sim 1$ s outburst in a 10-$M_{\odot}$ black hole binary. While some stellar mass Galactic systems do exhibit dramatic X-ray flares on such short time-scales (e.g. GRS 1915+105; Greiner, Morgan & Remillard 1996; Morgan, Remillard & Greiner 1997; Muno, Morgan & Remillard 1999), these systems do not return to quiescence immediately (if at all). To the best of our knowledge, there are no known stellar mass black hole binaries that transition from quiescence to Eddington luminosities on such a short time-scale. If PTF10iya is truly an AGN

outburst, it would suggest some new accretion physics that does not appear to manifest itself in stellar mass systems.

Regardless of its ultimate origin, it is clear that events like PTF10iya have not been previously reported. However, because of its short time-scale, this does not necessarily mean such outbursts are rare. Given the large luminosity (comparable to the brightest SNe), current and future optical surveys should be capable of detecting additional similar events out to relatively large distances, provided they observe with sufficiently high cadence. Rapid broadband follow-up observations will be key to uncovering more examples of this class (see e.g. Gal-Yam et al. 2011, for a detailed discussion of the PTF follow-up time-line).

## REFERENCES

Abazajian K. N. et al., 2009, ApJS, 182, 543
Abdo A. A. et al., 2010, ApJS, 188, 405
Ayal S., Livio M., Piran T., 2000, ApJ, 545, 772
Bade N., Komossa S., Dahlem M., 1996, A&A, 309, L35
Baldwin J. A., Phillips M. M., Terlevich R., 1981, PASP, 93, 5
Becker R. H., White R. L., Helfand D. J., 1995, ApJ, 450, 559
Beckmann V., Engels D., Bade N., Wucknitz O., 2003, A&A, 401, 927
Blandford R. D., Rees M. J., 1978, in Wolfe A. M., ed., BL Lac Objects. University of Pittsburgh Press, Pittsburgh, PA, p. 328
Bloom J. S. et al., 2009, ApJ, 691, 723
Bloom J. S. et al., 2011a, Sci, 333, 203
Bloom J. S. et al., 2011b, PASP, preprint (arXiv:1106.5491)
Bower G. C., 2011, ApJ, 732, L12
Brandt W. N., Pounds K. A., Fink H., 1995, MNRAS, 273, L47

Bregman J. N., 1990, A&AR, 2, 125
Brown P. J. et al., 2009, AJ, 137, 4517
Bruzual G., Charlot S., 2003, MNRAS, 344, 1000
Burrows D. N. et al., 2005, Space Sci. Rev., 120, 165
Burrows D. N. et al., 2011, Nat, 476, 421
Butler N. R., 2007, AJ, 133, 1027
Calzetti D., 2001, PASP, 113, 1449
Cannizzo J. K., 1993, ApJ, 419, 318
Cenko S. B. et al., 2006, PASP, 118, 1396
Cenko S. B. et al., 2011, ApJ, preprint (arXiv:1107.5307)
Colgate S. A., 1974, ApJ, 187, 333
Djorgovski S. G. et al., 2008, Astron. Nachr., 329, 263
Donley J. L., Brandt W. N., Eracleous M., Boller T., 2002, AJ, 124, 1308
Drake A. J. et al., 2009, ApJ, 696, 870
Ellis R. S. et al., 2008, ApJ, 674, 51
Elvis M., Page C. G., Pounds K. A., Ricketts M. J., Turner M. J. L., 1975, Nat, 257, 656
Esquej P., Saxton R. D., Freyberg M. J., Read A. M., Altieri B., Sanchez-Portal M., Hasinger G., 2007, A&A, 462, L49
Esquej P. et al., 2008, A&A, 489, 543
Evans C. R., Kochanek C. S., 1989, ApJ, 346, L13
Evans P. A. et al., 2007, A&A, 469, 379
Ferrarese L., Merritt D., 2000, ApJ, 539, L9
Filippenko A. V., 1982, PASP, 94, 715
Filippenko A. V., 1997, ARA&A, 35, 309
Fossati G., Celotti A., Ghisellini G., Maraschi L., 1997, MNRAS, 289, 136
Fossati G., Maraschi L., Celotti A., Comastri A., Ghisellini G., 1998, MNRAS, 299, 433
Frank J., Rees M. J., 1976, MNRAS, 176, 633
Gal-Yam A., Ofek E. O., Filippenko A. V., Chornock R., Li W., 2002, PASP, 114, 587
Gal-Yam A. et al., 2011, ApJ, 736, 159
Gebhardt K. et al., 2000, ApJ, 539, L13
Gehrels N. et al., 2004, ApJ, 611, 1005
Gelino D. M., Harrison T. E., Orosz J. A., 2001, AJ, 122, 2668
Gezari S., Halpern J. P., Komossa S., Grupe D., Leighly K. M., 2003, ApJ, 592, 42
Gezari S. et al., 2006, ApJ, 653, L25
Gezari S. et al., 2008, ApJ, 676, 944
Gezari S. et al., 2009, ApJ, 698, 1367
Ghez A. M. et al., 2008, ApJ, 689, 1044
Giannios D., Metzger B. D., 2011, MNRAS, 416, 2102
Goodrich R. W., 1989, ApJ, 342, 224
Greiner J., Morgan E. H., Remillard R. A., 1996, ApJ, 473, L107
Greiner J., Schwarz R., Zharikov S., Orio M., 2000, A&A, 362, L25
Grupe D., Beuermann K., Mannheim K., Bade N., Thomas H., de Martino D., Schwope A., 1995, A&A, 299, L5
Grupe D., Wills B. J., Leighly K. M., Meusinger H., 2004, AJ, 127, 156
Grupe D., Leighly K. M., Komossa S., 2008, AJ, 136, 2343
Halpern J. P., Filippenko A. V., 1988, Nat, 331, 46
Heckman T. M., 1980, A&A, 87, 152
Heckman T. M., Ptak A., Hornschemeier A., Kauffmann G., 2005, ApJ, 634, 161
Hills J. G., 1975, Nat, 254, 295
Ho L. C., 2008, ARA&A, 46, 475
Ho L. C., Filippenko A. V., Sargent W. L. W., 1997, ApJS, 112, 315
Horne K., 1986, PASP, 98, 609
Immler S., Lewin W. H. G., 2003, in Weiler K., ed., Supernovae and Gamma-Ray Bursters. Springer-Verlag, Berlin, p. 91
Jordi K., Grebel E. K., Ammon K., 2006, A&A, 460, 339
Kaiser N. et al., 2002, in Tyson J. A., Wolff S., eds, SPIE Conf. Ser. Vol. 4836, Survey and Other Telescope Technologies and Discoveries. SPIE, Bellingham, p. 154
Kasliwal M. M. et al., 2010, ApJ, 723, L98
Kauffmann G. et al., 2003a, MNRAS, 341, 33
Kauffmann G. et al., 2003b, MNRAS, 346, 1055
Kennicutt R. C., 1998, ARA&A, 36, 189

Kewley L. J., Dopita M. A., 2002, ApJS, 142, 35
King A. R., Pounds K. A., 2003, MNRAS, 345, 657
Komossa S., Bade N., 1999, A&A, 343, 775
Komossa S., Greiner J., 1999, A&A, 349, L45
Komossa S., Böhringer H., Huchra J. P., 1999, A&A, 349, 88
Kormendy J., Richstone D., 1995, ARA&A, 33, 581
Kulkarni S. R., Rau A., 2006, ApJ, 644, L63
Lacy J. H., Townes C. H., Hollenbach D. J., 1982, ApJ, 262, 120
Lauer T. R. et al., 2007, ApJ, 662, 808
Law N. M. et al., 2009, PASP, 121, 1395
Levan A. J. et al., 2011, Sci, 333, 199
Li L., Narayan R., Menou K., 2002, ApJ, 576, 753
Li W., Jha S., Filippenko A. V., Bloom J. S., Pooley D., Foley R. J., Perley D. A., 2006, PASP, 118, 37
Lodato G., King A. R., Pringle J. E., 2009, MNRAS, 392, 332
McHardy I. M., Papadakis I. E., Uttley P., Page M. J., Mason K. O., 2004, MNRAS, 348, 783
McHardy I. M., Koerding E., Knigge C., Uttley P., Fender R. P., 2006, Nat, 444, 730
Magorrian J. et al., 1998, AJ, 115, 2285
Maksym W. P., Ulmer M. P., Eracleous M., 2010, ApJ, 722, 1035
Malkan M. A., Sargent W. L. W., 1982, ApJ, 254, 22
Maoz D., 2007, MNRAS, 377, 1696
Maoz D., Nagar N. M., Falcke H., Wilson A. S., 2005, ApJ, 625, 699
Matheson T., Filippenko A. V., Ho L. C., Barth A. J., Leonard D. C., 2000, AJ, 120, 1499
Menou K., Quataert E., 2001, ApJ, 552, 204
Modjaz M. et al., 2009, ApJ, 702, 226
Morgan E. H., Remillard R. A., Greiner J., 1997, ApJ, 482, 993
Muno M. P., Morgan E. H., Remillard R. A., 1999, ApJ, 527, 321
Ofek E. O. et al., 2010, ApJ, 724, 1396
Ohsuga K., Mori M., Nakamoto T., Mineshige S., 2005, ApJ, 628, 368
Oke J. B., Gunn J. E., 1983, ApJ, 266, 713
Oke J. B. et al., 1995, PASP, 107, 375
Osterbrock D. E., 1989, Astrophysics of Gaseous Nebulae and Active Galactic Nuclei. University Science Books, Mill Valley, CA
Osterbrock D. E., Pogge R. W., 1985, ApJ, 297, 166
Peng C. Y., Ho L. C., Impey C. D., Rix H.-W., 2002, AJ, 124, 266
Phinney E. S., 1989, in Morris M., ed., Proc. IAU Symp. 136, The Center of the Galaxy. Kluwer, Dordrecht, p. 543
Pian E., Romano P., Maoz D., Cucchiara A., Pagani C., Parola V. L., 2010, MNRAS, 401, 677
Piran T., 2005, Rev. Mod. Phys., 76, 1143
Poole T. S. et al., 2008, MNRAS, 383, 627
Poznanski D. et al., 2010, Sci, 327, 58
Quimby R. M., Aldering G., Wheeler J. C., Höflich P., Akerlof C. W., Rykoff E. S., 2007, ApJ, 668, L99
Racusin J. L. et al., 2008, Nat, 455, 183
Rahmer G., Smith R., Velur V., Hale D., Law N., Bui K., Petrie H., Dekany R., 2008, in McLean I. S., Casali M. M., eds, SPIE Conf. Ser. Vol. 7014, Ground-based and Airborne Instrumentation for Astronomy II. SPIE, Bellingham, p. 70144Y
Ramirez-Ruiz E., Rosswog S., 2009, ApJ, 697, L77
Rau A. et al., 2009, PASP, 121, 1334
Rees M. J., 1988, Nat, 333, 523
Renzini A., Greggio L., di Serego Alighieri S., Cappellari M., Burstein D., Bertola F., 1995, Nat, 378, 39
Roming P. W. A. et al., 2005, Space Sci. Rev., 120, 95
Sanders D. B., Phinney E. S., Neugebauer G., Soifer B. T., Matthews K., 1989, ApJ, 347, 29
Sari R., Piran T., Narayan R., 1998, ApJ, 497, L17
Schlegel D. J., Finkbeiner D. P., Davis M., 1998, ApJ, 500, 525
Schmidt B. P., Keller S. C., Francis P. J., Bessell M. S., 2005, BAAS, 37, 457
Sérsic J. L., Pastoriza M., 1967, PASP, 79, 152
Shields G. A., 1978, Nat, 272, 706
Siemiginowska A., Elvis M., 1997, ApJ, 482, L9
Simcoe R. A., Metzger M. R., Small T. A., Araya G., 2000, BAAS, 32, 758

Skrutskie M. F. et al., 2006, AJ, 131, 1163

Smith N., Chornock R., Silverman J. M., Filippenko A. V., Foley R. J., 2010, ApJ, 709, 856

Soderberg A. M. et al., 2008, Nat, 453, 469

Spergel D. N. et al., 2007, ApJS, 170, 377

Strubbe L. E., Quataert E., 2009, MNRAS, 400, 2070

Strubbe L. E., Quataert E., 2011, MNRAS, 415, 168

Tremonti C. A. et al., 2004, ApJ, 613, 898

Ulmer A., 1999, ApJ, 514, 180

Urry C. M., Padovani P., 1995, PASP, 107, 803

van Velzen S., Farrar G. R., Gezari S., Morrell N., Zaritsky D., Ostman L., Smith M., Gelfand J., 2011a, ApJ, 741, 73

van Velzen S., Körding E., Falcke H., 2011b, MNRAS, L310

Veilleux S., Osterbrock D. E., 1987, ApJS, 63, 295

Voges W. et al., 1999, A&A, 349, 389

Wade R. A., Horne K., 1988, ApJ, 324, 411

Wehrle A. E. et al., 1998, ApJ, 497, 178

Wizinowich P. L. et al., 2006, PASP, 118, 297

Zauderer B. A. et al., 2011, Nat, 476, 425

This paper has been typeset from a TeX/LaTeX file prepared by the author.